DEVELOPMENT AND VALIDATION OF THE DELIQUESCENT RELATIVE HUMIDITY TEST METHOD FOR THE ACCUMULATED PARTICULATE MATTER FOUND IN A DATA CENTER UTILIZING AN AIRSIDE ECONOMIZER

by

ROSHAN ANAND

Presented to the Faculty of the Graduate School of

The University of Texas at Arlington in Partial Fulfillment

of the Requirements

for the Degree of

MASTER OF SCIENCE IN MECHANICAL ENGINEERING

THE UNIVERSITY OF TEXAS AT ARLINGTON

MAY 2018

Acknowledgements

I would like to take this opportunity to express my deepest gratitude to my supervising professor Dr. Dereje Agonafer for his remarkable support, guidance and continuous encouragement throughout the course of my research work. Working with him has been my greatest privilege.

I would like to thank Dr. Prabjit Singh for providing the multipurpose test boards that have been used in this study. His invaluable advice, expertise on various research areas and timely support whenever required has enabled me to successfully complete my research work.

Every result that is described in this thesis was accomplished with the help and support of my research team, Jimil M. Shah and Gautham Thirunavakkarasu. Their thought provoking ideas and motivation has helped me not just for my research work but also during the entire course of my graduate study. I would also like to thank Mr. Ankith John for always being there with words of encouragement and a listening ear.

I would now like to thank my parents Mr. N Anand Kumar and Mrs. Nalini Anand and my sister Ms. Shivani Anand for their unconditional love, constant support and blessings.

I owe a debt of gratitude to my best friend Ms. Aishwarya Mohan, and I would like to thank her for her advice, motivation and unyielding support. I would like to thank the Almighty for his never-ending grace, mercy and for keeping all circumstances in favor to me that has led me successfully defend my thesis.

April 26, 2018

Abstract

DEVELOPMENT AND VALIDATION OF THE DELIQUESCENCE RELATIVE HUMIDITY TEST METHOD FOR THE ACCUMULATED PARTICULATE MATTER FOUND IN A DATA CENTER UTILIZING AN AIRSIDE ECONOMIZER

Roshan Anand, MS

The University of Texas at Arlington, 2018

Supervising Professor: Dereje Agonafer

Data centers are virtual or physical infrastructure utilized by enterprises to house computer, server and networking systems and other vital components for the needs of the company's information technology mainly serving the purpose of storing, processing and serving large amounts of mission critical data to clients. As data centers house a network's most critical systems and are extremely vital for the continuity of daily operations, every organization prioritizes the reliability and security of data centers and their information.

A remarkable amount of data center energy is consumed in eliminating the heat generated by Information Technology (IT) equipment to maintain and ensure safe operating conditions and optimum performance. Therefore, energy efficient cooling of data centers is of utmost importance. Airside economization is being encouraged to reduce the associated cooling costs by limiting the operational hours of computer room air conditioning (CRAC) units. The installation of ASEs bears the risk of particulate contamination in data centers, hence, deteriorating the reliability of information technology (IT) equipment. The relative humidity (RH) has a significant effect on the physical form of the accumulated dust particles and in turn the safe operation of the IT

equipment. It is necessary and informational to have a clear understanding of the terms ‘Critical Relative Humidity (CRH)’ and the ‘Deliquescence Relative Humidity (DRH)’. CRH is defined as the relative humidity at which the salt or dust particles just begins to adsorb enough moisture to start becoming electrically conductive. DRH is defined as the relative humidity at which the salt or dust particles begin the formation of a saturated salt solution. When the RH in the data center exceeds the deliquescent relative humidity (DRH) of salts or accumulated particulate matter, it absorbs moisture, becomes wet and subsequently leads to electrical short circuiting because of degraded surface insulation resistance between the closely spaced features on the printed circuit boards (PCB’s). Another concern with this type of failure is the absence of evidence that hinders the process of evaluation and rectification. Therefore, it is imperative to develop a practical test method to determine the DRH value of the accumulated particulate matter found on PCB’s.

This thesis is a first attempt to develop and validate an experimental technique attempt to measure the DRH of dust particles by logging the leakage current versus %RH for the particulate matter dispensed on an interdigitated comb coupon.

To validate this methodology, the DRH of pure salts like Magnesium Chloride ($MgCl_2$), Ammonium Nitrate (NH_4NO_3) and Sodium Chloride (NaCl) is determined and their results are then compared with their published values. This methodology can therefore be implemented to help lay a modus operandi of establishing the limiting value or an effective relative humidity envelope to be maintained at a real-world data center facility for its continuous and reliable operation at its respective location.

Table of Contents

List of Illustrations

List of Tables

Chapter 1

Introduction

1.1 Data Centers and ASHRAE Guidelines

A repository that generally houses the core of an organization's information systems or computing facilities like servers, routers, switches and firewalls, also supporting components like backup equipment, fire suppression, smoke detection, air conditioning systems, raised floors for better cabling and prevention of water damage is what defines a typical data center.

Figure 1-1 depicts the power consumed by distinct components of a data center [1]. The cooling units, which comprise of the heating, ventilation and air conditioning (HVAC) fans and HVAC cooling are used for cooling and maintaining the temperature of Information Technology (I.T) equipment. This consumes an approximate 31% of the overall data center energy. Complete utilization of an economizer with changes in the operating temperature of the data center allows operators to save a monumental 74% of mechanical energy [2].

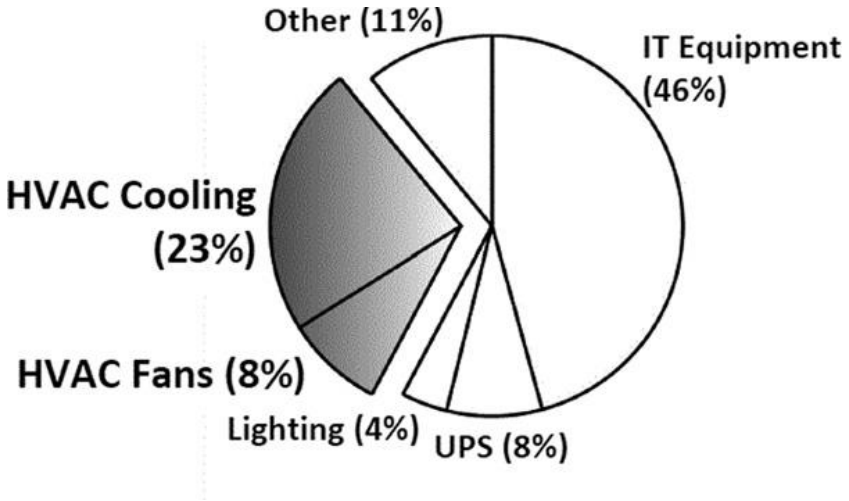

Figure 1-1 Power Allocation in a Data Center

With the unabating establishment of data centers all over the world, data center operators are often availing to cost reduction techniques such as allowing data centers to operate outside the recommended American Society of Heating, Refrigeration and Air-Conditioning Engineers (ASHRAE) envelope and employing airside economizers (ASEs) to tackle substantial cooling costs and increasing server densities. Data center administrators were also obliged by the ASHRAE TC9.9 subcommittee, on Mission Critical Facilities, Data Centers, Technology Spaces, and Electrical Equipment, to allow data centers to operate outside the recommended temperature-humidity range, i.e. into allowable classes A1-A3 [3]. The ASHRAE A3 envelope, under severe conditions, allows the electronic equipment to operate for short yet unrestricted periods of time at temperature and humidity levels as high as 24^{o}C and 85% relative humidity.

Figure 1-2 shows the recommended and allowable temperature-humidity, as defined in the 3rd edition of the 'ASHRAE Thermal Guidelines for Data Processing Environments' published in 2012, that should be considered by the information technology (I.T) manufacturers [4].

The employment of ASEs gives rise to the concept called free cooling. Ambient outdoor air is utilized to cool the I.T equipment directly, thereby curtailing the chiller operation when the air is sufficiently cool and dry. Information and communication companies, including companies like Google, Microsoft and Intel are adopting free air cooling methods as a means of reducing greenhouse gas emissions and energy costs [5] [6]. Though ASEs play a vital role in eliminating the need for mechanical cooling, they risk the entry of particulate contaminants that could result in contamination related hardware failure.

There is an increase in power density because of shrinkage in the feature size of electronic devices. Thus, the equipment cabinets are to be provided with enhanced

cooling that is frequently accomplished by using forced air. Accumulation of particulate matter or dust particle deposition increases up to 100 times as the velocity of air across the surfaces is increased [7]. Accumulated particulate matter is unarguably a critical factor that greatly effects the reliability of I.T equipment.

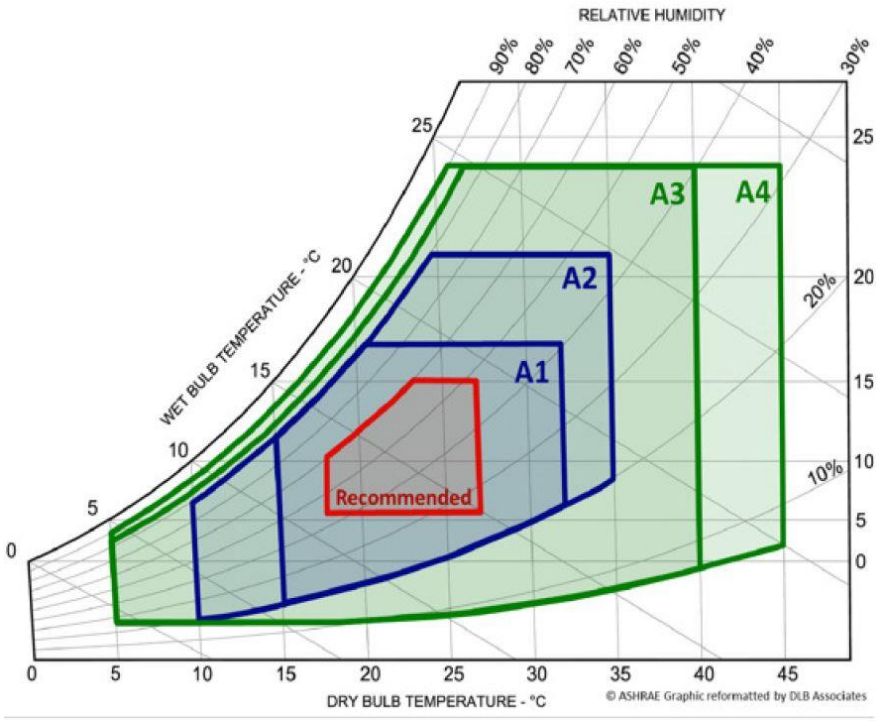

Figure 1-2 ASHRAE recommended and allowable ranges to an IT equipment manufacturer.

1.2 Airside Economization

To diminish the data center energy consumption due to chiller operations, airside economizers (ASE) are employed partially or completely when ambient air conditions are favorable. ASHRAE defines an air economizer as “A duct and damper arrangement and

automatic control system that together allows a cooling system to supply outdoor air to reduce or eliminate the need for mechanical cooling during mild or cold weather [8].” This efficient cooling method draws in outside air from the ambient and is then filtered using MERV 11 or MERV 13 filters to eliminate particulate contaminants before being introduced into the cold aisle of a data center. When the temperature of the outside air is lower than the temperature of the air that is recirculated in the data center, the economizer mixes it with the exhaust air (hot air) to achieve the desired temperature and humidity range. The mixed air is then supplied to the data center with proper filtration and conditioning. The amount of enthalpy in the air is acceptable and no auxiliary conditioning is required if the outside air is both sufficiently cool and dry. This mode of cooling operation is generally termed as free cooling [9]. Free cooling is adopted by numerous data centers across the United States as displayed in Figure 1-3 which also shows the usage of airside economizers in hours per year.

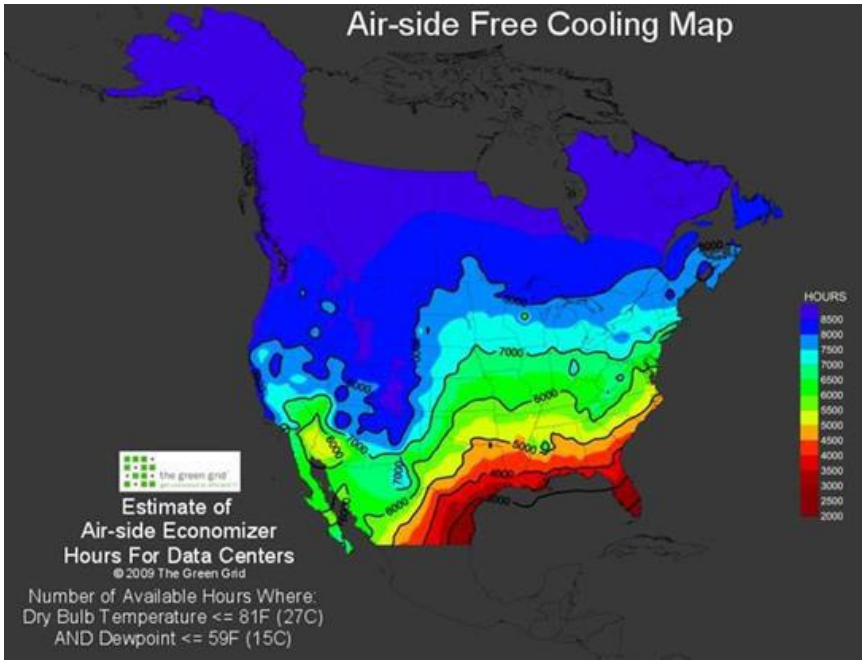

Figure 1-3 Usage hours of an airside economizer under ideal conditions

Utilization of ASEs result in the significant reduction in energy consumption of a data center in association with the cooling infrastructure. The risk that comes with the use of ASEs is that the temperature and humidity levels must be within specified ranges and more importantly is the entry of particle and gaseous contaminants that should be within allowable ranges. Direct evaporative cooling (DEC), indirect evaporative cooling (IEC), or two-stage indirect/direct evaporative cooling (I/DEC) systems could also be used to condition the outside air to increase the number of working hours of the ASE.

Figure 1-4 shows the schematic of an airside economizer and Figure 1-5 depicts the working operation of an airside economizer.

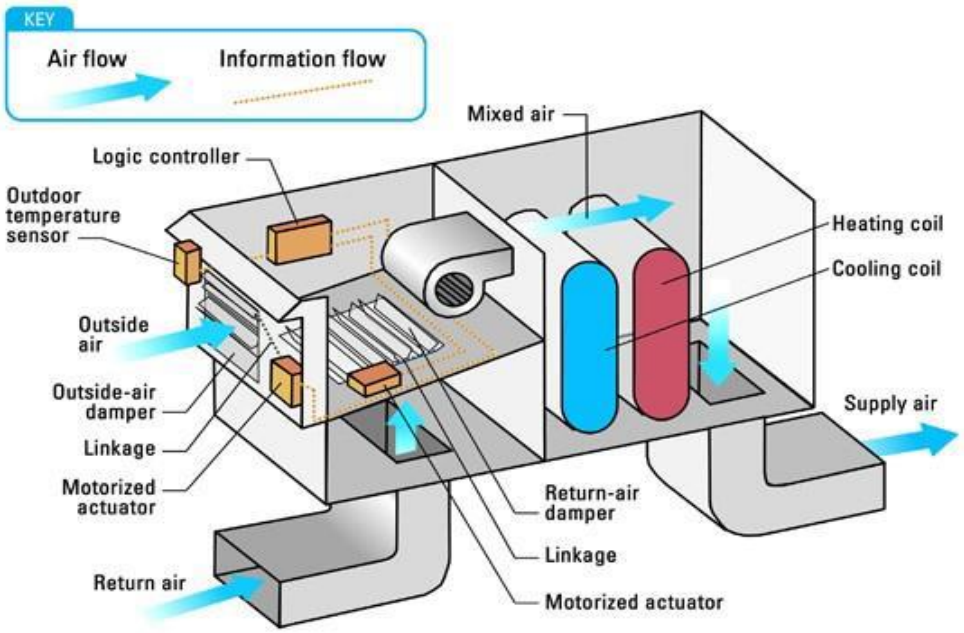

Figure 1-4 Airside Economizer

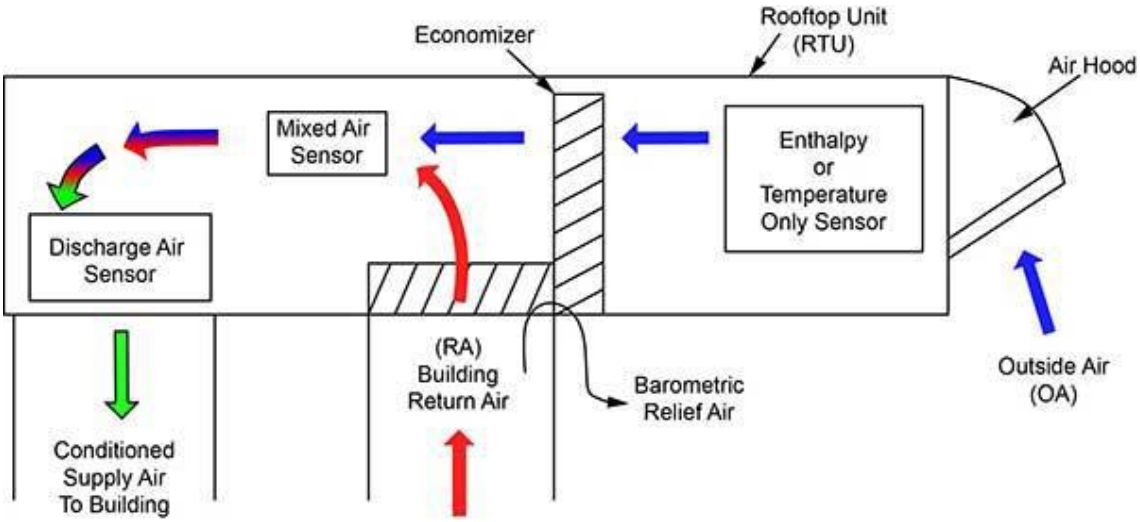

Figure 1-5 Working of an airside economizer

1.3 Effect of the Physical Environment on IT Equipment Reliability

The physical environment that surrounds the IT equipment is mainly defined by the temperature, relative humidity and gaseous and particulate contaminants. These factors can have adverse effects on IT equipment and can cause its failure in two ways:

- Corrosion of silver termination in surface mount components results in the formation of electrical open circuits. This type of failure mode occurs mainly in geographical areas with high levels of sulphur bearing gaseous contaminants [10]. Manufactures continue to improve their hardware to tackle this failure mode.
- There are also a few other mechanisms that result in electrical short circuits. (i) In 2006, the European Union's RoHS directive banned the use of lead in solders. This led to changes in the surface finish of PCBs [11]. This also led to increased failure rates of PCBs because of creep corrosion [12,13]. (ii) Electrochemical

reactions such as ion migration and cathodic and anodic filamentations [14]. (iii) Particulate matter that settles on PCBs adsorb moisture thereby reducing surface insulation resistance between the closely spaced features on PCBs.

This thesis mainly deals with the study of particulate contaminants and the role and effect of particulate contaminants under the influence of relative humidity.

Chapter 2

Dust or Particle Contamination

2.1 Introduction

Fine, dry particulate matter mainly composed of particles of the earth or waste material lying on the ground or on different surfaces or carried in air in defined as dust. There are numerous terms used synonymously with dust such as atmospheric dust, particulate contamination, particulate matter and airborne particles. In terms of its characteristics and compositions, dust is known to have a complex nature and understanding.

Based on their size, dust is mainly classified into two groups: fine particles and coarse particles. Fine particles are defined as particles with a diameter less than or equal to 2.5μm such as those found in diesel particulate matter (DPM), exhaust of motor vehicles, smoke and haze. Fine particles are further classified into primary and secondary particles [15,16]. Primary particles are the fine particles that are directly emitted from a specific source, such as volcanoes, forest fires, unpaved roads, construction sites, fields, etc. Secondary fine particles are those that are formed because of photochemical reactions that take place in the atmosphere and make up most of the fine particulate pollution. These photochemical reactions occur due to the presence of oxides of sulphur and nitrogen that are emitted from automobiles and various industries. Carbonaceous material with a size of less than 0.1μm interact with nitrogen dioxide and sulphur dioxide in a multistep photochemical process to thereby result in the formation of nitric and sulfuric acids. Fertilizers generally containing ammonia, decayed biological matter and other sources neutralize these acids thereby forming ammonium sulphate, ammonium nitrate and ammonium hydrogen sulphate. Most of these secondary particles are considered anthropogenic [17,18]. On the other hand, coarse particles are those particles

with a size range of 2.5-15μm. They include sea salt, natural and artificial fibres and plant pollen. Their major sources mainly include erosion of soil, flaking of biological materials and minerals [19].

Dust particles consists of both organic and inorganic substances. The inorganic substances generally outweigh the organic substances. Certain inorganic compounds are water soluble salts. Table 2-1 lists the relative content of the main mineral particles in dust. Methods like X-ray power diffraction (XRPD), transmission electron microscopy (TEM) and electron probe microanalysis (EPMA) have been implemented to analyze the mineral [20].

Table 2-1 Relative Content of Mineral Particles Found in Dust

Minerals	**Main Compositions**	**Relative Contents**	
		Nature dust (size < 250 μm)	**Fine particles (Size <10 μm)**
Quartz	SiO_2	1	1
Feldspar	$KAlSi_3O_8$-$NaAlSi_3O_8$-$CaAl_2Si_2O_8$	0.77	0.8
Calcite	$CaCO_3$	0.48	1.91
Mica	$SiO_2 \cdot Al_2O_3 \cdot K_2O \cdot Na_2O \cdot H_2O$	0.41	2.24
Gypsum	$CaSO_4 \cdot 2H_2O$	0.05	0.72

Fibres, carbon black and organic ions such as acetate ($CH3COO^-$) and formate ($COOH^-$) are the organic substances in dust [21]. These organic compounds can be analyzed by gas chromatography or mass spectrometry (GC/MS). Thermo gravimetric analysis (TGA) is used to evaluate the weight percentage of organic compounds.

When considering the impact of dust on the reliability of IT equipment, the focus is mainly imparted on the ionic content of dust particles because they have the tendency to dissolve in water and conduct electricity. When dust begins to adsorb moisture and when it eventually forms a saturated solution, the major cations and anions are Na^{+}, NH^{4+}, K^{+}, Ca^{2+}, Mg^{2+}, Cl^{-}, NO^{3-}, F^{-} and $SO4^{2-}$ [22].

In coarse particles, calcium, ammonium, sulphate, sodium, magnesium and chloride are the most common ionic components with large local variations for sodium, magnesium and chloride [23].

2.2 Properties of Accumulated Particulate Matter

- **Thermal Conductivity:** Solid dust particles that accumulate on the equipment creates a thermal insulating layer and thus minimizes the allocated area for heat dissipation. This leads to the excessive heating up of components.
- **Electrical Conductivity:** Solid substances can be classified into highly insulating substances and electrically conducting substances. Insulating substances aid in accumulating static charges destroys the working on integrated circuits. When the relative humidity is considerable high, these substances can absorb moisture and can subsequently lead to their increased conductivity thus causing hardware failures.
- **Abrasiveness:** Particulate matter that deposit between moving parts can result in their wear and tear over time.
- **Adhesiveness:** This is generally defined as the ability of particulate matter to stick or hold on to the surface. This furthers leads to an increase in the thickness of the thermal layer, bearing failures and high voltage relays.

- **Corrosivity:** The nature of dust particles permits them to ingest moisture and vaporous contaminants and thus become corrosive [24].

Two extremely common consequences of particulate or dust contaminations on printed circuit boards are electrochemical migration and loss of impedance, i.e. the loss of surface insulation resistance, between traces and component leads. These two failure mechanisms involve the contamination by creating a path flow for leakage current.

Chapter 3

Dust Related Failure Mechanisms

3.1 Surface Insulation Resistance (SIR) and Electrochemical Migration (ECM)

Accumulated particulate matter or dust drastically increases the risk of several failure modes in PCBs. Moisture sorption by hygroscopic materials in dust and the capillary action by mineral particles lead to the formation of a thick water film on the substrate of PCBs. The water-soluble salts that are present in the dust dissolve in the water film thereby causing ionic contamination. This in turn results in the reduction in surface insulation resistance (SIR) to an unacceptable limit by forming a conductive path across adjacent electrodes. In other words, SIR degradation on a printed circuit board occurs between the electrical conductors when they are connected by a substrate that is covered by an electrolyte formed by hygroscopic particulate matter or dust at elevated relative humidity conditions. The PCB includes certain metals such as copper traces, solder materials and component leads. The ionic contamination can react with these metals on the board and can result is the dissolution of the metal which can corrode the metal. Under the influence of an electric field, certain metallic ions dissolved in the anode could migrate to the cathode to form metallic dendrites. This mode of failure is termed as electrochemical migration (ECM). An electric field is one of the main driving forces in ECM. The metal dendrites bridge the gap between adjacent conductors or features thus causing the leakage current between these conductors to increase. Permanent failures can take place if a dendrite carries current density and leads to a permanent short. When a dendrite grows, causes an electrical short and then a burn out due to high localized current density, intermittent failures occur. The propensity of ion migration also depends on the solubility of the corrosion products at the anode. Metal compounds having lower

solubility give out fewer ions for migration. Corrosion and ECM are accompanied by leakage current failure that is measured as SIR degradation. PCBs that have dust settled on them might fail at an early stage due to reduction in SIR between the closely spaced features in the presence of moisturized dust (appropriate RH conditions close to the DRH), before the dendrites bridge.

Figure 3-1 displays a schematic representation of electrochemical migration according to the ‘classical model’ [25]. The dissolved Mn+ ions at the anode migrate to the cathode. At the cathode, they are deposited by receiving electrons and reducing back to metal. This ‘classical model’ was initially demonstrated for the migration of silver [26]. It was later proved that this model could also be applied to many other metals that are used in electronics such as copper, tin and lead [27].

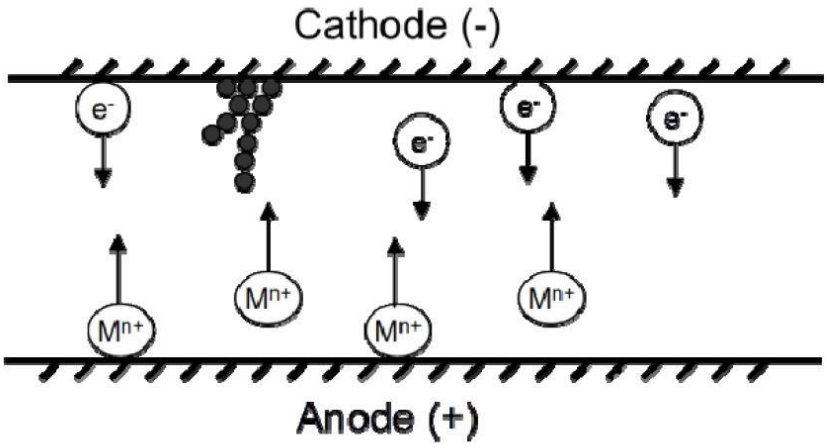

Figure 3-1 Schematic Representation of the ECM Phenomenon

The growth of dendrites take place when electrolyte bridges two electrodes and forms a path. Anodic dissolution results in the formation of metal ions. At the anode, cations are

generated due to oxidation of metals and causes anodic corrosion. Under the influence of electromotive forces, the metal ions migrate through the electrolyte towards the cathode and the last step is the electrochemical metal deposition at the cathode. Dendrites or dendrite like structures may continue to grow towards the anode as more neutral metal deposits on the nuclei. When the dendrite runs through the entire gap between the two adjacent conductors and makes contact with the anode, an electrical short might occur. As a result of Joule heating, the current flowing through the dendrite could burn out a part of the dendrite. This situation can cause intermittent failures. If the dendrites that form are thick enough to withstand the current flowing through it, it can result in a permanent short [28].

Chapter 4

Relative Humidity

4.1 Role of relative Humidity

Relative humidity can significantly influence IT. They are as follows [29]:

- Deteriorated performance of IT equipment through increased dissipation factor and PCB epoxy dielectric constant.
- The presence of gaseous contamination leads to enhanced corrosion.
- Decrease in the surface insulation resistance in the presence of particulate contamination.

4.2 Concept of CRH and DRH

In simple terms, relative humidity (RH) is defined as the amount of water vapor in the air and is generally expressed as a percentage of the maximum amount that the air could hold at the given temperature. Critical Relative Humidity (CRH) is defined as the relative humidity at which the salt or dust particles just begins to adsorb enough moisture to start becoming electrically conductive. Deliquescence Relative Humidity (DRH) is defined as the relative humidity at which the salt or dust particles begin the formation of a saturated salt solution.

When dust settles on PCBs, it can lead to an electrical short circuiting between closely spaced features when a voltage drop exists across them. This corrodes the circuit board components and metal traces. The ionic components in the dust absorb moisture from the environment and creates ionic bridges which result in the electrical short circuiting. The presence of moisture in the air and ionic components in the dust together leads to corrosion. Besides affecting the reliability of equipment by corrosion and ion migration,

dust can also degrade computer reliability due to overheating by settling around electrical connectors.

When the humidity in the environment rises above the deliquescence relative humidity of the particulate matter, it is known to become wet and therefore ionically conductive and corrosive [30]. Miniaturization of electronic of electronic components, the decrease in the feature spacing on printed circuit boards and allowing in the data center to operate in allowable temperature and relative humidity ranges in order to save energy is making electronic hardware susceptible to failure due to accumulation of particulate matter.

The plot of electrical conductivity of the particulate matter versus relative humidity can be best used to best describe the role of particulate contamination in high relative humidity environments on hardware reliability [30]. The electrical conductivity can be expressed as the leakage current through the accumulated particulate matter when a constant voltage across the particulate matter exists. Figure 4-1 shows an example of a graph of the log of leakage current versus relative humidity for a certain amount of particulate matter collected from IT equipment from a certain data center in India [29]. The CRH is estimated at the intersection of the lower relative humidity asymptote and the inversion line. This is the relative humidity at which the particulate matter just begins adsorbing enough moisture to start becoming electrically conductive. The intersection of the inversion line with the upper asymptote corresponds to the value of the deliquescent relative humidity (DRH) of the particulate matter. This value of relative humidity is at which the formation of a saturated salt solution begins. Particulate matter of low deliquescence relative humidity is of major concern. They could either be generated within the data center space or its source could be outside air. The fine particles and ultrafine particles that are present in the outside air are high in ionic content in the form of ammonium, sulphate and nitrate salts. Generation of particulate matter within a data

center with low DRH is extremely rare. The water is high in salt content, magnesium chloride being the most damaging. In humidifiers that are poorly maintained, the salt content present in the water begins to escalate. Once the water spray droplets evaporate, they leave behind a salt residue that then becomes airborne as the air passes through the humidifier. This salt settles on IT equipment and in turn causes hardware failure in the presence of high relative humidity. The rusting of the nickel-plated steel covers on various subassemblies right above the raised floor is usually the first indication of the presence of corrosive salts and high relative humidity. These perforated steel covers are the inlet for the cold air high in humidity. This problematic situation can be prevented by installing a reverse osmosis system in the humidifier thus keeping the humidifier water low in ionic content.

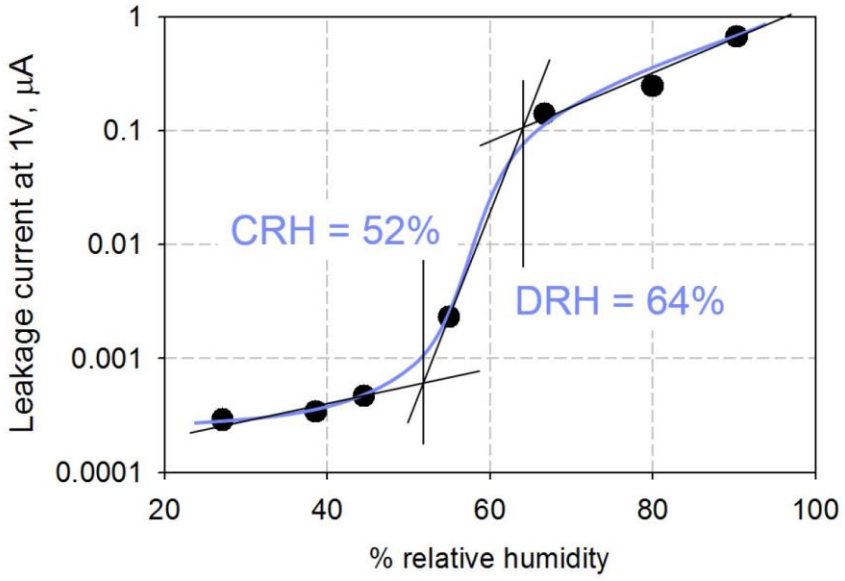

Figure 4-1 Leakage current through accumulated particulate matter as a function of relative humidity.

4.3 DRH Measurement Techniques

The most important parameter controlling the rate of corrosion is the relative humidity in the data center. Each salt contamination has a certain value of deliquescent relative humidity beyond which the salt will absorb moisture and become wet. Wet salts can further corrode metals. Therefore, it is imperative to develop a practical test method to determine the DRH value of the accumulated particulate matter found on PCB's.

With respect to the measurement of Deliquescent Relative Humidity of pure salts, there are two other experimental methodologies. They are:

- Gravimetric Method
- Electrical Impedance Method

4.3.1 Gravimetric Method:

This method focuses on measuring the weight of the salt at different values of relative humidity. With a plot of the weight of the salt Vs %RH, the DRH of the salt can be determined. This plot can also be termed as a growth curve for salt particles. A microgravimetric balance is employed is measuring the weight of the salt. The ideology behind this method comes with the adsorbing nature and hence the increase in the weight of the salt sample. Thus, the value of relative humidity at which there is a sudden change in the weight of the salt is said to be its DRH value.

Certain amount of the salt sample is placed an aluminum pan and is kept in a dynamic vapor sorption apparatus at a temperature of 25^{o}C. The chamber is the evacuated to a vacuum to make sure the sample is completely dry and free of any moisture content. A mass flow controller unit is utilized to introduce water vapor into the measurement chamber until the desired value of relative humidity is obtained. The microbalance aids in monitoring the weight of the salt sample throughout the experiment. The relative humidity was varied between 0%-90% with an interval of 2%.

The following figure, Figure 4-2, shows the mass change or the mass uptake of a few salts (NaCl and NH_4NO_3) and varying values of relative humidity [30]. In other words, the mass uptake of the salts is compared as a function of relative humidity. Below a certain threshold relative humidity, the mass uptake of each salt is almost negligible which agrees completely with the theory as well. It can also be seen that the leakage current is also extremely low below a certain relative humidity. It is only after a certain %RH that the there is a significant rise in the mass uptake or water adsorbed by the salt. The value of leakage current can also be seen to rise steeply beyond this threshold value. The results obtained in this method, i.e. DRH for NaCl as 73% and the DRH for NH_4NO_3 as 58% are below their published values of 75% and 62%-64% respectively.

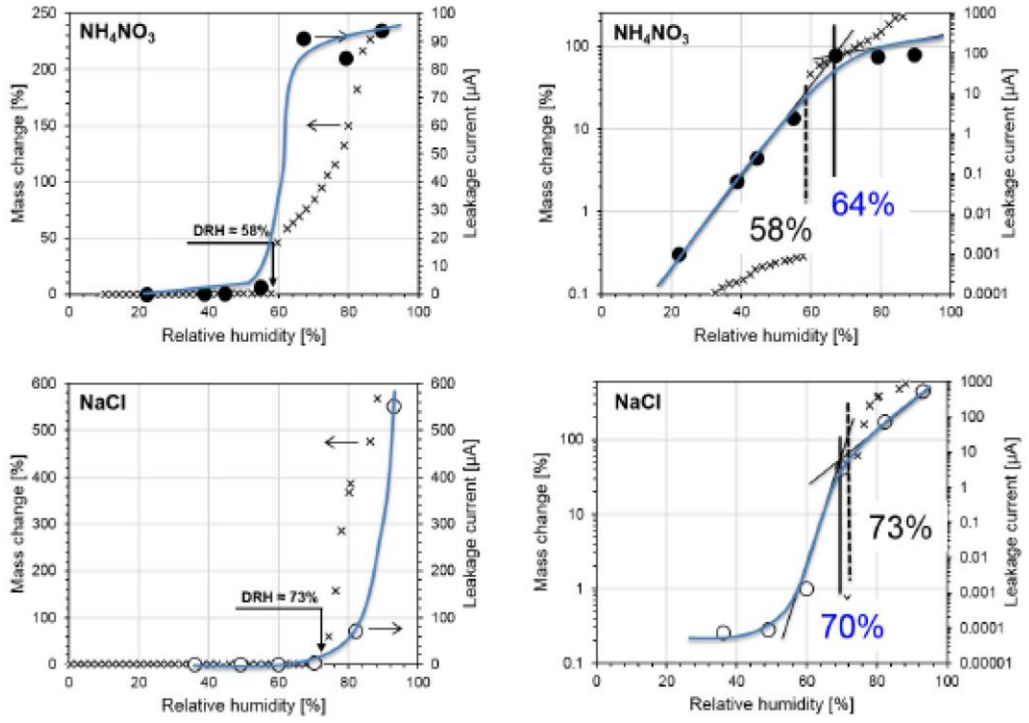

Figure 4-2 Gravimetric Method compared to the leakage current method at 25°C for NH_4NO_3 and NaCl: Linear and Logarithmic Graphs.

Limitations of this Method:

- Salts have the tendency to actively react with the environment that surrounds it. It is very important to make sure that the chamber is completely void of any moisture content at the beginning of the experiment. Since this method focuses on the mass change as a function of DRH, it is imperative to be extremely cautious with the experimental setup.
- The step range is 2% of relative humidity. Only when the change in mass over time becomes negligible for a certain value of relative humidity, the sample is considered to be in a state of equilibrium with the water vapor and only then its mass is recorded. Thus, this method would take a much longer time to give out results and thus determine the corresponding DRH of the salt.
- Despite the small step range, the intensive care of the testing equipment, incorporation of more data points and time investment, yet the results obtained by this method do not match the published values.

4.3.2 Electrical Impedance Method

The experimental setup for this method of DRH measurement is as shown in Figure 4-3. A conductivity cell that comprises of two platinum electrodes and a piece of porous paper is used for the DRH measurement of the salt sample. The porous paper is wetted with the salt solution to help develop an evenly distributed layer of salt crystals to form between the platinum electrodes when the relative humidity is lower than the DRH [31].

The porous paper or filtration paper is placed on a surface that is arched and that is made of polytetrafluoroethylene (PTFE). At values above the DRH of the salt, the salt adsorbs the moisture and forms a solution, the arched allows this excess liquid to drain off and thus maintain a constant thickness of the conducting layer [32]. About 0.5mL of

the salt solution is carefully pipetted onto the filtration paper before starting the experiment.

A precision impedance analyzer (LCR Meter) is utilized in this experiment as a conductivity measuring meter. The alternating current voltage frequency is set at 1000Hz. At frequencies higher than 1000 Hz, poor response was noted. A data acquisition system is coupled to the LCR mater and the controller of the humidity chamber.

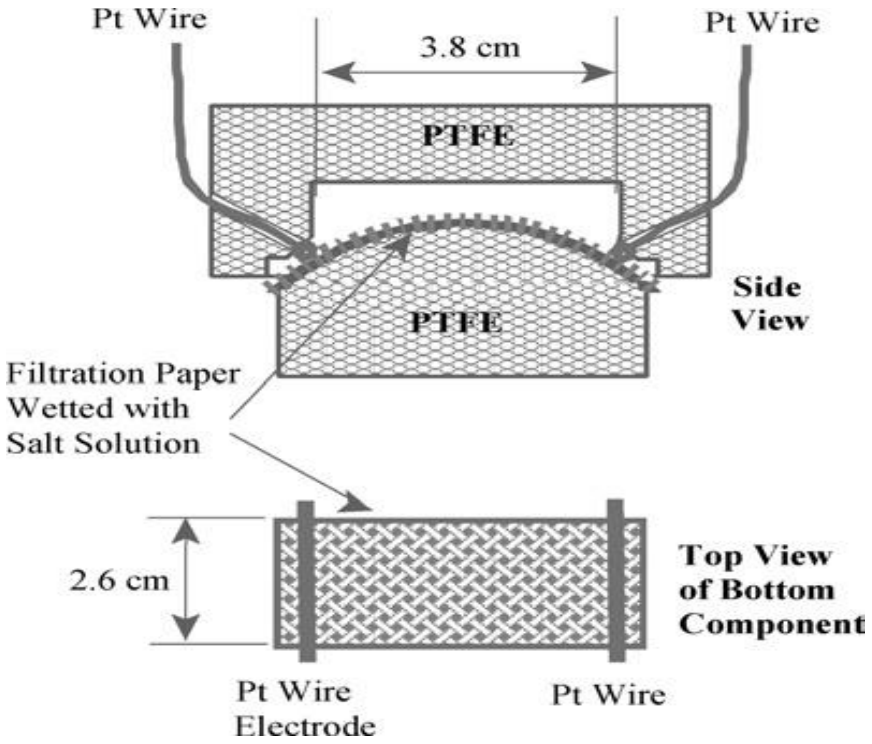

Figure 4-3 Schematic diagram of the conductivity cell for DRH Measurement

The experiment conducted in this study was used to determine the electrical impedance of the conductivity cell containing Na_2SO_4 (Sodium Sulphate). Figure 4-4 shows how the impedance of the conductivity cell varies with increasing values of %RH. The experiment was conducted at a temperature of 50^{o}C and relative humidity varying from 78%-91%. Each step is carried out an interval of 23 hours. From the graph of impedance Vs %RH,

we can notice that the impedance decreases sharply as the %RH is increased from 85% to 88%. After 91%, the impedance remains unchanged. From this we can infer that the salt has reached its deliquesced state.

The sharp decrease in the electrical impedance as the %RH is increased from 85%-88% indicates that the DRH of Na_2SO_4 is between 85-88% at 50°C. Another fundamental factor that this method doesn't clearly explain is that the gradual decrease in measured impedance could also be likely due to the adsorption of water by the salt and not necessarily the deliquescence of the salt. As a result of deliquescence, an aqueous phase with a much lower impedance than that shown in Figure 4-4 would be formed.

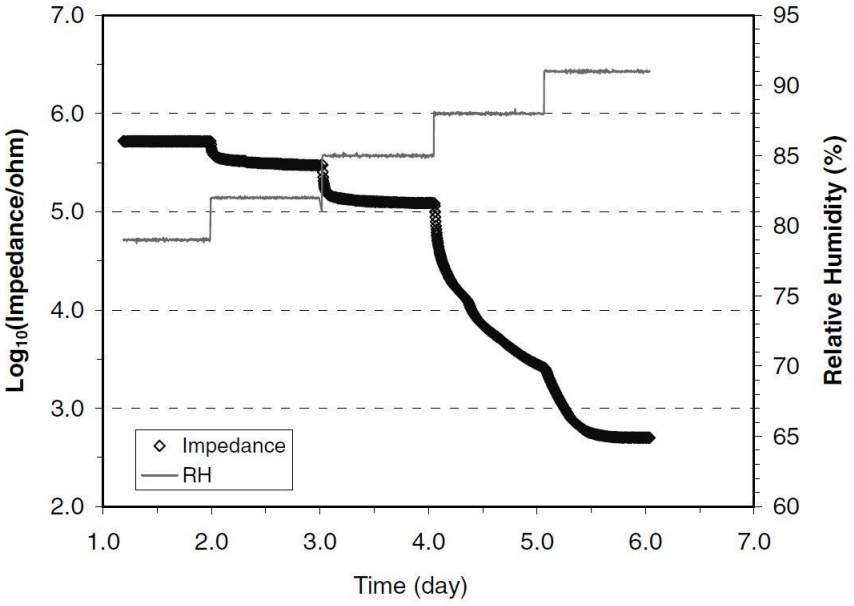

Figure 4-4 Impedance measured Vs %RH at 50°C (Na_2SO_4)

Limitations of this Method:

- Platinum electrodes and Data Acquisition Units are used thus making this experimental setup very expensive.
- Each time step is carried out an interval of 23 hours thereby making this process time consuming.
- The setup is a complicated and should not be disturbed.
- The results obtained have to further substantiated with concrete literature to help validate the technique.

Chapter 5

Experimental Method to Determine the DRH of Pure Salts

5.1 Experimental Requirements

This experiment aims at determining the deliquescence relative humidity (DRH) of pure salts. Since this experimental is the first of its kind, it is imperative to validate the experimental process by comparing the experimental results obtained with published results. This method is adopted based on the well-established relationship between the leakage current and %RH. The influence of particulate matter on the reliability of I.T. equipment can be described by a plot of the electrical conductivity of particulate matter against relative humidity.

The following items are used in order to help develop this experimental method to determine the DRH of pure salts and thus accomplish the objectives of this thesis.

5.1.1 Salt Solutions

- Three salt solutions, namely: Sodium Chloride (NaCl), Ammonium Nitrate (NH_4NO_3), Magnesium Chloride ($MgCl_2$) are used in this experiment to determine their DRH.
- 0.1 wt% of each of the salt solution is prepared. 10mg of the salt is dissolved in 10ml of deionized water thus resulting in the 0.1 wt% concentration. The DRH of the salt is doesn't vary with its concentration.
- Deionized water is generally defined as water that is free from all charged atoms or molecules or ions. Also, deionized water is commonly used in performing this experiment because the ions found in water can affect the experiment.

Incorporation of ions in the experiment, even in a small amount, can produce faulty or inaccurate results.

Figure 5-1 shows the three salt solutions – Sodium Chloride, Ammonium Nitrate and Magnesium Chloride respectively.

Figure 5-1 Sodium Chloride, Ammonium Nitrate and Magnesium Chloride Solution

At a temperature of 25^{o}C, the following are the published DRH values of each salt [33]:

- Sodium Chloride: 75.8%
- Ammonium Nitrate: 64%
- Magnesium Chloride: 32.78%

Certain information of some ions found in these salt soultions are discussed.

Chloride Ions(Cl^-)

One of the most detrimental materials found in dust is chloride. Chlorides accelerate the electrochemical failure mechanisms such as electrolytic corrosion and metal migration when combined with moisture in the environment and an electrical bias.

The amount of chloride added by the soldering process to bare PCBs was investigated by Weekes [34]. It was shown the 3 µg/in^2 was added to the bare printed circuit boards by using no-clean flux and about 8µg/in^2 was added by using water soluble flux. Ion chromatography (IC) and SIR were conducted to dtermine the acceptable amount of chloride on assembled boards and on bare boards. It was found that about 2.5 µg/in^2 and µg/in^2 were the acceptable amounts when using no clean flux when using bare boards and assembled boards respectively. When using water soluble flux, 6 µg/in^2 and 8 µg/in^2 were acceptable amounts.

Ammonium Ions (NH_4^+)

The chemical reaction of ammonia (NH_3) with hydrogen ions could result in the formation of ammonium. Ammonium (NH_4^+) is mildly acidic. Ammoium has the tendency to complex with hydroxide ions resulting in the formation of hydrogen ions thus leading to an acidic environment. Most ammonium salts are highly soluble in water. The limiting ionic

conductivity of ammonium ions is 73.7 $S.cm^2/mol$ [35], making it equally conductive as the chloride and potassium ions. The presence or existence of ammonium ions can decrease the SIR of PCBs in the presence of moisture.

Sodium Ions (Na^+)

Since the standard electrode electrode potential of sodium relative to the standard hydrogen electrode potential is -2.71 V, the sodium metal is highly reductive [35]. It is because of this particular reason why sodium exists in the environment never as a free element but only as a compound.

The sodium ions (Na^+) are highly stable in water. They always exist as counter ions to numerous anions, sodium chloride (NaCl) being the most abundant. The limiting value of ionic conductivity of the sodium ions is 50.11 $S.cm^2/mol$ which is two-thirds that of chloride ions (Cl^-). Thus the existence of Na^+ in the surface moisture film can lower the SIR and greatly increase the conductibity of PCBs.

5.1.2 Multipurpose Test Board

To specifically evaluate and understand the interactions between the solder masks, solder paste and fluxes, the Institute for Printed Circuits, also called the IPC, designed the ‘IPC-B-25A Multipurpose Test Board’ or the ‘PCB-B-25A Test Board’. Another vital function of this test board is to evaluate the effects of moisture and insulation resistance of solder masks.

The test board is normally a 0.062" FR-4. FR-4 is a NEMA (National Electrical Manufacturers Association) grade designation for the glass reinforced epoxy laminate material. This composite material is composed of woven fiberglass cloth with an epoxy resin binder that is flame resistant.

The board is a developed by a simple print and etch technique. Also, the available surfaces are bare copper, Electroless nickel immersion gold (ENIG) or hot air solder levelling (HASL) for materials qualification. It could also be any other surface finish as required.

Two comb patterns from the IPC-B-24 test board were included in the IPC-B-25A test board are designated as patterns E and F. The pattern D was included from the IPC-B-25 board, which was the older board and identical to pattern B/E. Pattern C which is the military Y pattern, was used to link to extensive qualification databases in the military.

Figure 5-2 shows the IPC-B-25A Multipurpose Test Board that is used in this experimental method. The comb coupons E and F are specifically used for this experiment.

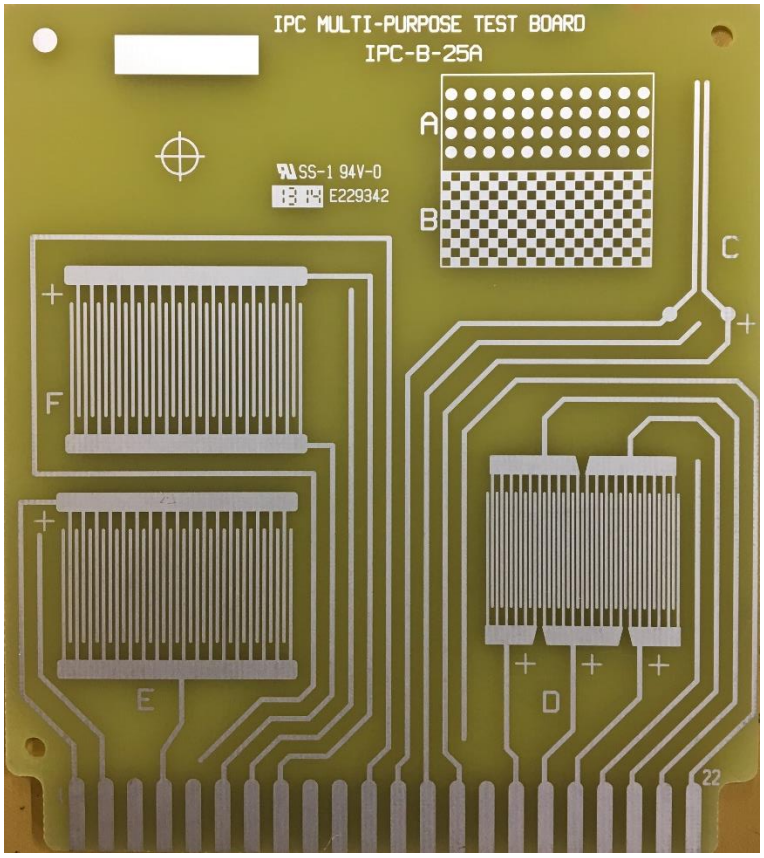

Figure 5-2 IPC-B-25A Multipurpose Test Board

5.1.3 Environmental Chamber

For this experiment, the temperature was maintained at 25ºC and the relative humidity was varied from 10%-90% at regular time intervals of 1 hour and 30 minutes between each step. In order to perform this operation, the 'Thermotron SE-600-10-10 Environmental Chamber is used. Figure 5-3 shows the environmental chamber used in this experiment

Figure 5-3 Environmental Chamber – Thermotron SE-600-10-10

The Thermotron incorporates a wide range of applications and specific compressor selections ranging from 3 to 15 Hp. It can provide rapid product temperature changes. The optimized airflow system of the Thermotron improves gradient control thereby providing greater accuracy, tighter uniformity and enhanced performance on the products.

The Thermotron is equipped with a 12" touch screen programmable controller therefore making data collection and operation of the chamber easy and reliable. With respect to the functions executed in the experiment, the following are a few chamber capabilities.

- Workspace Volume: 20.7 ft^3
- Humidity Range: 10% - 98%
- Temperature Range: -70^oC – 180^oC

5.1.4 D.C Power Supply

This experiment requires a very precise application of 1 volt. The ‘Agilent E3614A’ power source serves the purpose. The constant voltage (CV) mode is used to provide the desired 1V. Figure 5-4 shows the D.C. power source that is employed. In addition to the constant voltage and constant current modes, there also exists an adjustable over-voltage protection, front and rear output terminals, remote analog programming and remote sensing that helps in automatically compensating the voltage drops.

Figure 5-4 D.C Power Supply

5.1.5 INA-219 Current Sensor coupled with an Arduino Uno Board

In order to help measure the leakage current which falls in the mA range, the Adafruit INA-219 current sensor is employed. This current sensor is coupled with an Arduino Uno board. A program is developed to help this setup accurately measure and display the value of leakage current at each instant when voltage is applied across the ends of each comb coupon. The INA-219 board helps in obtaining solutions for all power monitoring problems keeping the margin of error less than 1%. Figure 5-5 displays the current sensor with the screw terminal [36].

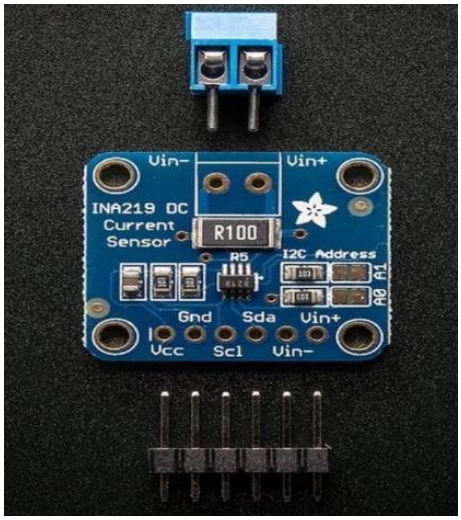

Figure 5-5 INA219 Current Sensor

Of the many Arduino boards that are currently available in the market, the Arduino Uno as shown in Figure 5-6, is the most commonly used open-source microcontroller board. The Arduino Uno board consists of a 16MHz quartz crystal, a power jack, a reset button, 6 analog pins and 14 digital pins that can be interfaced to various other circuits or expansion boards. The Arduino Integrated Development Environment (IDE) is used to

program the Arduino Uno via a USB cable. An external 9V battery or a USB cable can be used to power the Arduino. It also accepts voltages between 7 and 20V.

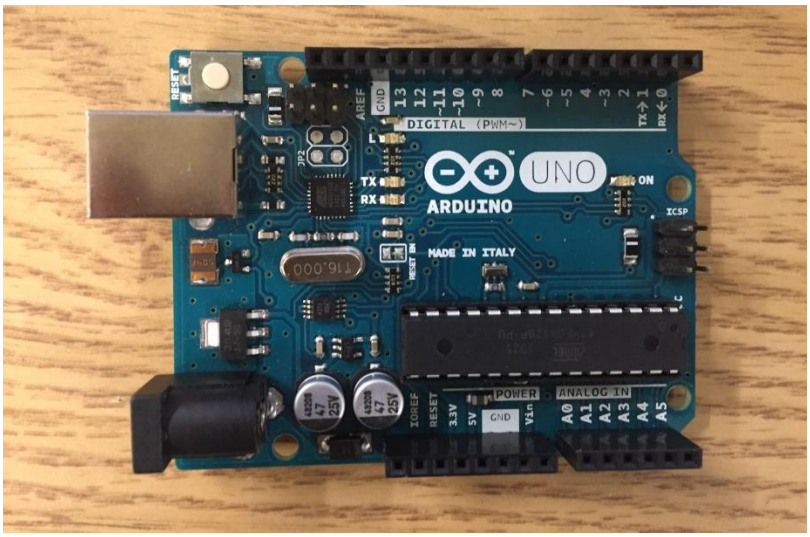

Figure 5-6 Arduino Uno

Coupling the Arduino and Current Sensor:

The 5V pin on the Arduino can be used to power up the INA219 current sensor breakout board. The sensor communicates with the Arduino via the I2C. Dupont cables are used to make the interconnects between the Arduino and the INA219 current sensor thereby allowing them to freely communicate. The interconnects made are as follows:

- The GND of the Arduino is connected to the GND of the sensor.
- The 5V of the Arduino is connected to VCC of the sensor.
- The SDA of the Arduino is connected to the SDA of the sensor.
- Lastly, the SCL of the Arduino is connected to the SCL of the sensor.

The schematic representation is as shown in Figure 5-7.

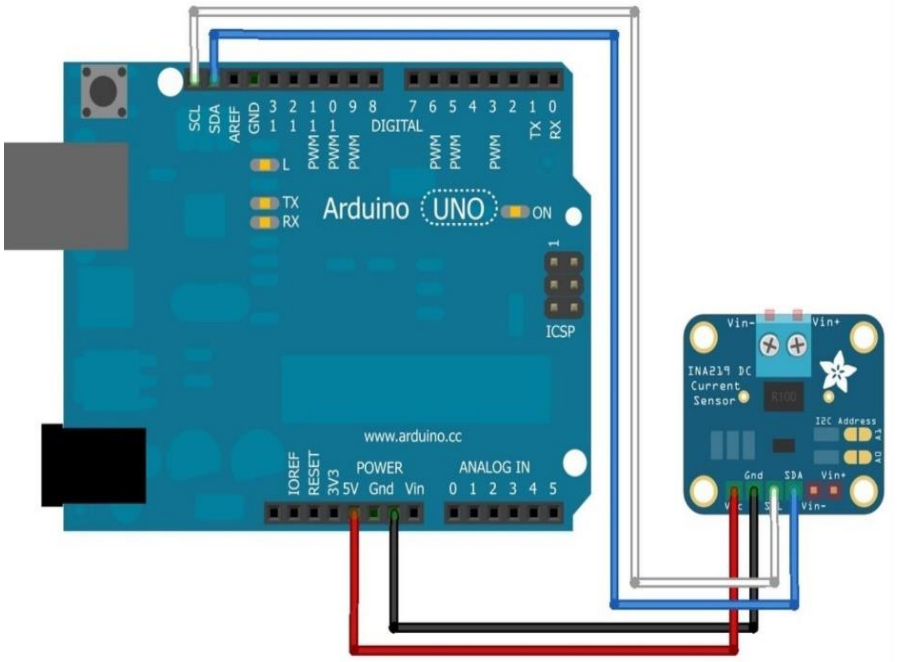

Figure 5-7 Interconnections between the Arduino and the INA219 Current Sensor

Development of the electrical circuit by assimilation of the current sensor:

Figure 4-5 also shows a screw terminal that is connected to soldered to the INA219 current sensor. The V+ of the screw terminal is connected to the positive terminal of the Agilent power source that is used. The V- of the screw terminal is connected to the positive terminal of the load. This helps in putting the sense resistor in line with the circuit. In this experiment, the connecting wire is soldered to the positive terminal of the load. Lastly, a connecting wire from the negative terminal of the power supply is connected to the GND on the Arduino and a connecting wire from the negative terminal of the power supply is soldered to the negative terminal of the load. Figure 5-8 shows the coupling of the sensor to the Arduino.

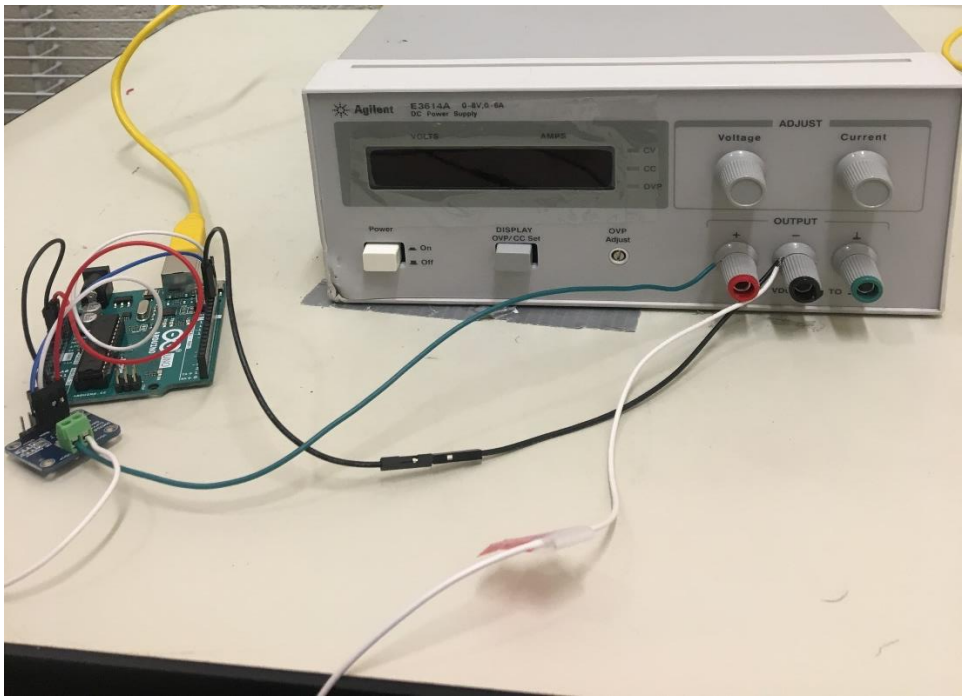

Figure 5-8 Arduino Coupled with the INA219 Current Sensor connected to the DC Power Source.

5.2 Experimental Procedure

- The soldering of the connecting wires and the interconnections between the Arduino and the current sensor is done as mentioned in section 5.1.5. The comb coupon is then placed in the environmental chamber as shown in Figure 5-9.

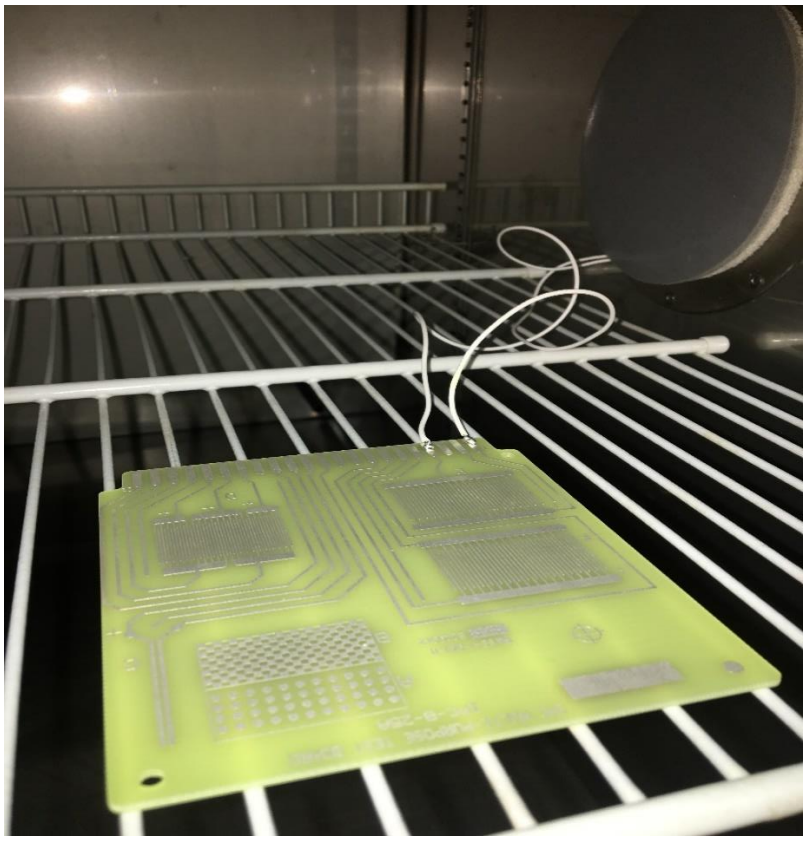

Figure 5-9 Connecting wires soldered to the positive and negative terminal of the comb coupon and place in the environmental chamber.

- 10 drops of the 0.1 wt% of the salt solution is carefully dispensed on the comb coupon using a suction syringe. A pipette can also be used. Figure 5-10 displays the salt solution dispensed on the comb coupon. One salt sample is tested at a time to ensure a controlled approach.

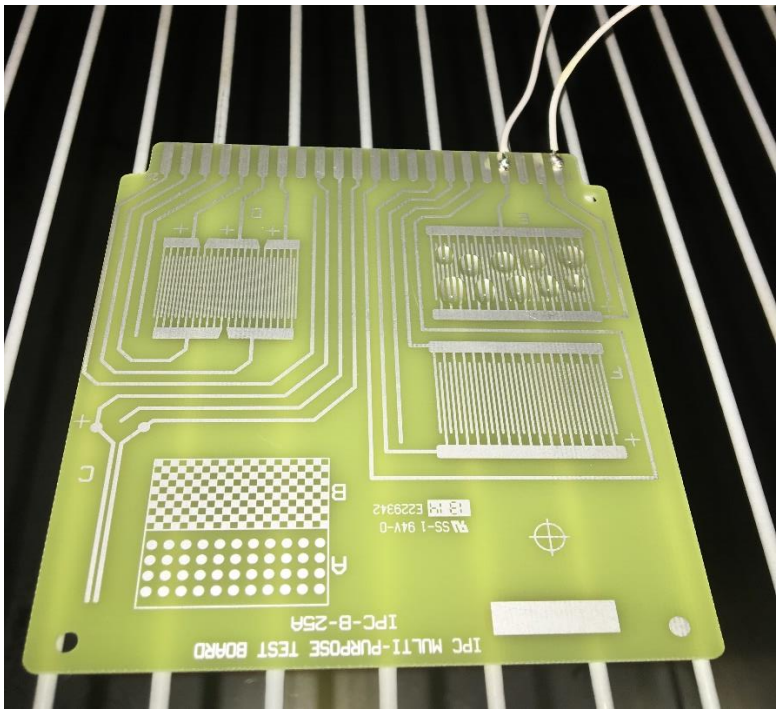

Figure 5-10 10 drops of the salt solution carefully dispensed on the comb coupon.

- It is very important to make sure that the comb coupon remains in the environmental chamber during the entire course of the experiment. The salts tend to quickly react or reach equilibrium conditions with the environment that surrounds it. Therefore, it is vital that the coupon remains untouched and undisturbed during the entire course of the experiment to obtain accurate results.
- The environmental chamber is then set to a fixed temperature of 25^{o}C and a relative humidity of 10% and is allowed to rest for a period of 12 hours. This step is performed to allow the saturated salt solution to get rid of its moisture content thereby allowing just the salt particles to settle on the coupon. At this step, the salt should be completely dry and free of moisture. Figure 5-11 displays the

programmable monitor of the environmental chamber displaying the value of temperature and %RH in the chamber.

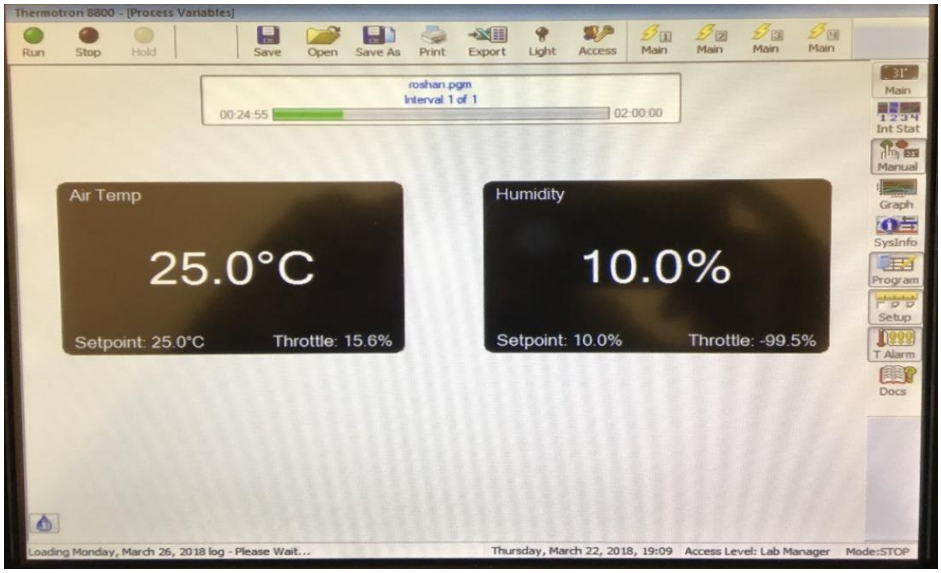

Figure 5-11 Touchscreen programmable monitor of the environmental chamber set at a temperature of 25^{o}C and 10% RH.

- A DC voltage of +1V and -1V, each for 1-2 seconds, is passed through the comb coupon to disturb the electrochemistry of the salt that is being tested. The reason to apply the -1V immediately after the application of +1V is to neutralize or cancel the effect of the +1V on the ions of the salt.

  The application of the positive and negative voltage is carried out by switch the connecting wires at the terminals of the power supply.
- Simultaneously, at this point, the leakage current is measured across the comb coupon. The INA219 current sensor coupled with the Arduino Uno board helps in displaying the load voltage and leakage current.

- The relative humidity is gradually increased in steps of 10% for a duration of 90 minutes each. This allows the salt to attain equilibrium with the relative humidity conditions. The load voltage and leakage current is measured again.
- This process is repeated until a relative humidity of 90% is achieved.
- The values of %RH, Leakage current (in mA) and Log of leakage current are tabulated.
- A graph of the log of leakage current is plotted versus the %RH.
- This plot helps in attaining the CRH and DRH of the respective salt that is being tested.
- The experiment is repeated for the remaining salt samples.

Chapter 6

Results and Discussions

6.1 Results

6.1.1 To estimate the DRH of Sodium Chloride (NaCl)

Table 6-1 displays the values of leakage current obtained at various values of %RH on the application on +1V and -1V respectively. The log of leakage current is also calculated and tabulated.

Table 6-1 Leakage current at varying values of %RH on the application of +1V and -1V (NaCl Sample)

+1 Volt			-1 Volt		
%RH	Current (mA)	Log I	%RH	Current (mA)	Log I
10	0.08	-2.52573	10	0.09	-2.40795
20	0.1	-2.30259	20	0.1	-2.30259
30	0.1	-2.30259	30	0.1	-2.30259
40	0.1	-2.30259	40	0.2	-1.60944
50	0.2	-1.60944	50	0.2	-1.60944
60	0.3	-1.20397	60	0.3	-1.20397
70	6.8	1.916923	70	8.1	2.091864
80	58.8	4.074142	80	64.6	4.168214
90	120	4.787492	90	129	4.859812

Figure 6-1 and 6-2 displays the linear plots of leakage current versus %RH when +1V and -1V have been applied respectively.

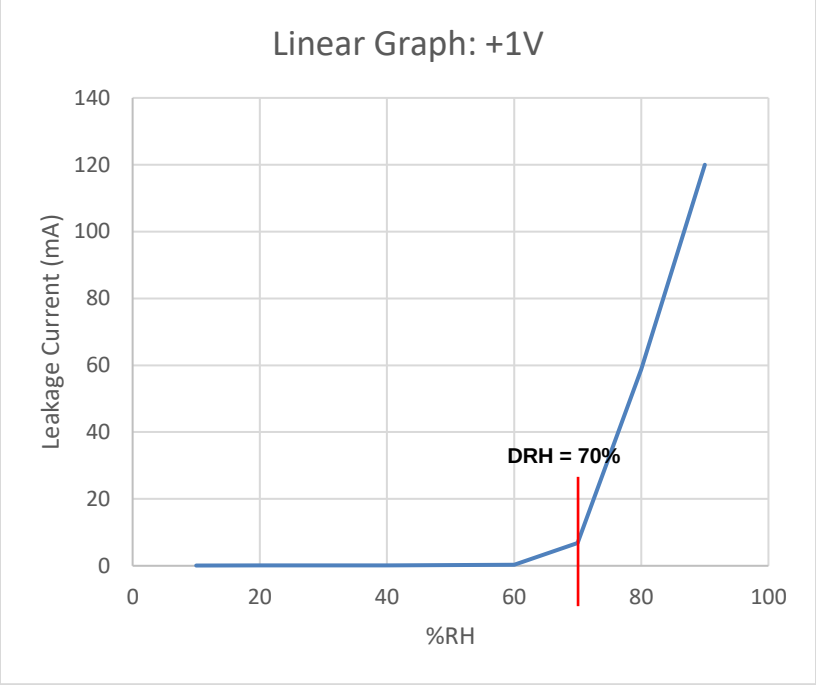

Figure 6-1 Linear plot of Leakage Current versus %RH for NaCl (+1 Volt)

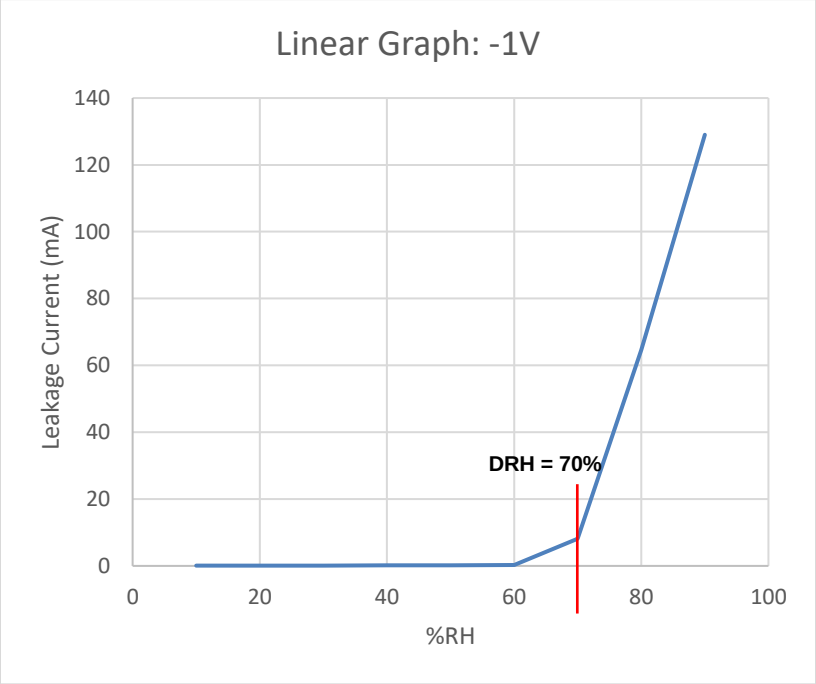

Figure 6-2 Linear plot of Leakage Current versus %RH for NaCl (-1 Volt)

Figure 6-3 and 6-4 displays the logarithmic plots of leakage current versus %RH when +1V and -1V have been applied respectively.

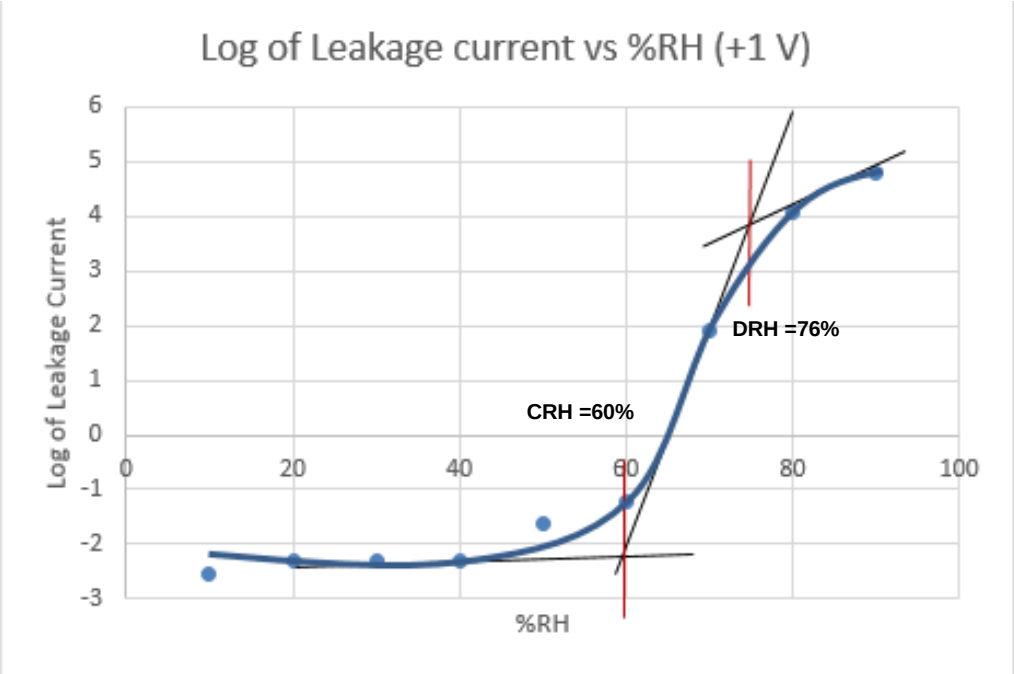

Figure 6-3 Logarithmic plot of Leakage Current versus %RH for NaCl (+1 Volt)

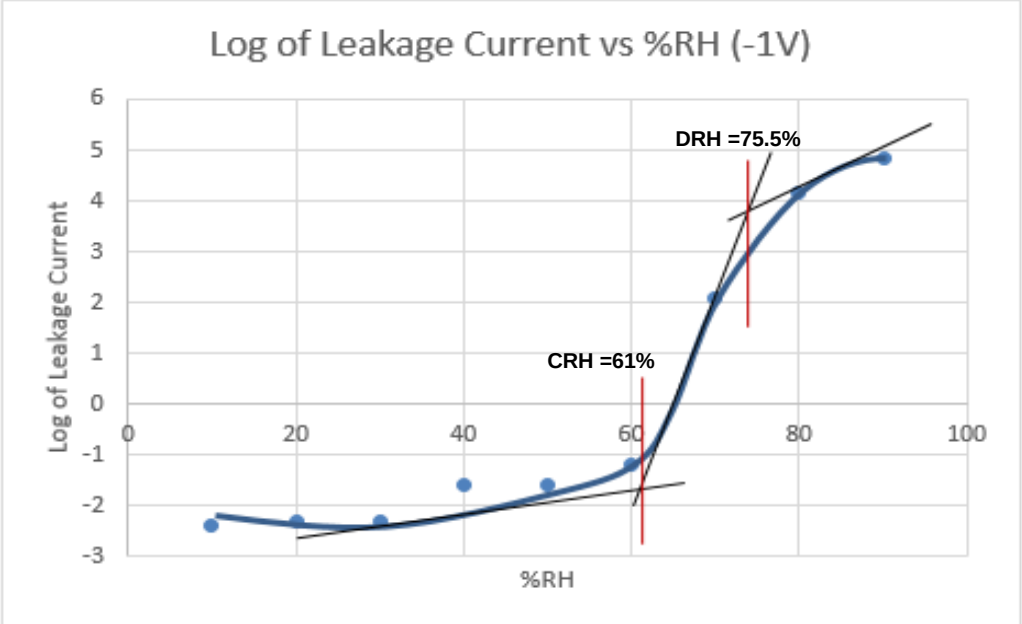

Figure 6-4 Logarithmic plot of Leakage Current versus %RH for NaCl (-1 Volt)

At the beginning of the experiment, few drops of the salt solution are dispensed on the coupon and is made to dry out completely before the stepwise increment in the %RH. During the course of the experiment, when the %RH exceeds the DRH of the salt, it begins to corrode the coupon. The before and after pictures of the comb coupon dispensed with NaCl solution is as seen in Figure 6-5 and Figure 6-6 depicts the effect of relative humidity in the presence of particulate contamination. The corrosion effects are also very evident.

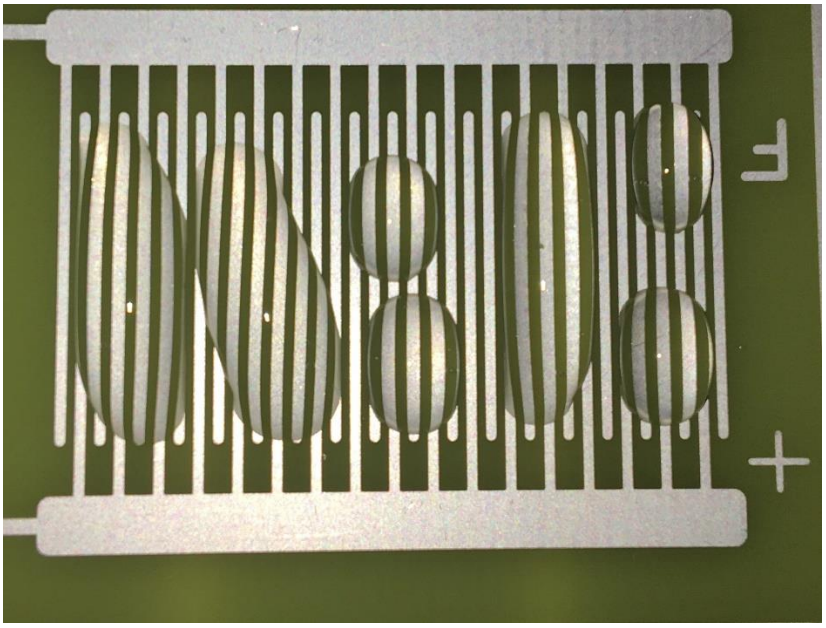

Figure 6-5 Drops of NaCl dispensed on the comb coupon.

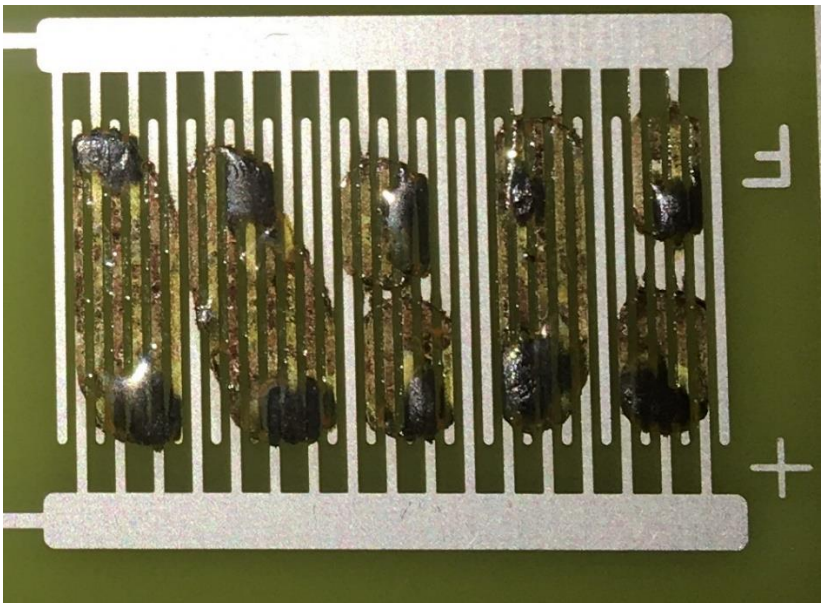

Figure 6-6 Corrosion due to the conducting nature of the NaCl salt solution at a relative humidity higher than the DRH.

6.1.2 To estimate the DRH of Ammonium Nitrate (NH_4NO_3)

Table 6-2 displays the values of leakage current obtained at various values of %RH on the application on +1V and -1V respectively. The log of leakage current is also calculated and tabulated.

Table 6-2 Leakage current at varying values of %RH on the application of +1V and -1V (NH_4NO_3 Sample)

+1 Volt			-1 Volt		
%RH	I (mA)	Log I	%RH	I (mA)	Log I
10	0.07	-2.65926	10	0.08	-2.52573
20	0.09	-2.40795	20	0.09	-2.40795
30	0.1	-2.30259	30	0.1	-2.30259
40	0.2	-1.60944	40	0.1	-2.30259
50	0.2	-1.60944	50	0.2	-1.60944
60	0.4	-0.91629	60	0.4	-0.91629
70	21.1	3.049273	70	21.1	3.049273
80	38.2	3.642836	80	38.2	3.642836
90	47	3.850148	90	47	3.850148

Figure 6-7 and 6-8 displays the linear plots of leakage current versus %RH for the ammonium nitrate sample when +1V and -1V have been applied respectively.

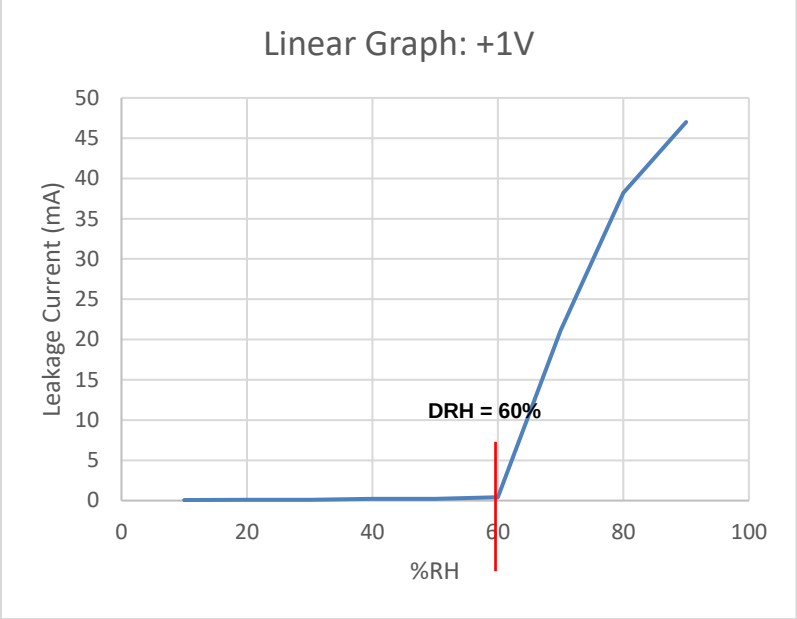

Figure 6-7 Linear plot of Leakage Current versus %RH for NH_4NO_3 (+1 Volt)

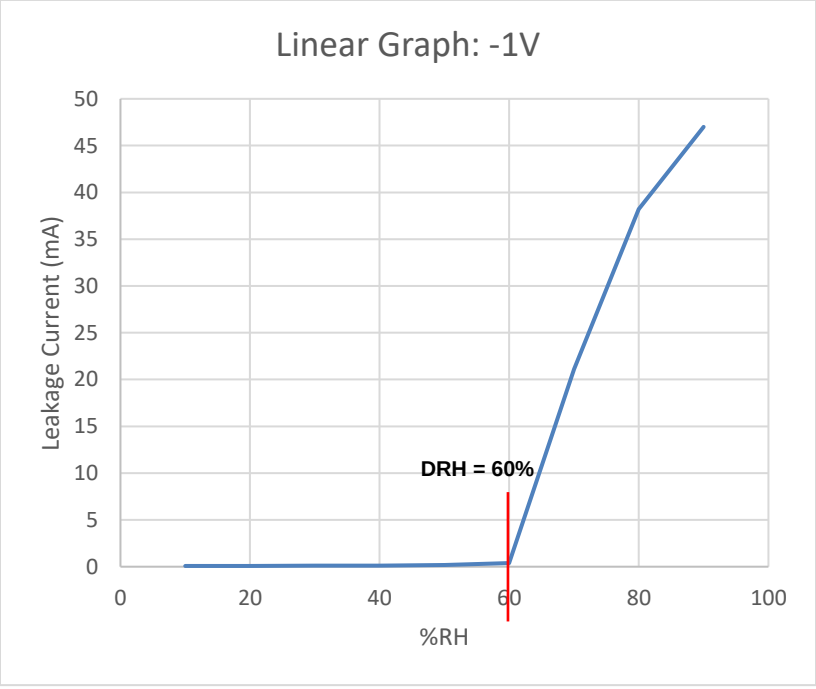

Figure 6-8 Linear plot of Leakage Current versus %RH for NH_4NO_3 (-1 Volt)

Figure 6-9 and 6-10 displays the logarithmic plots of leakage current versus %RH when +1V and -1V have been applied respectively.

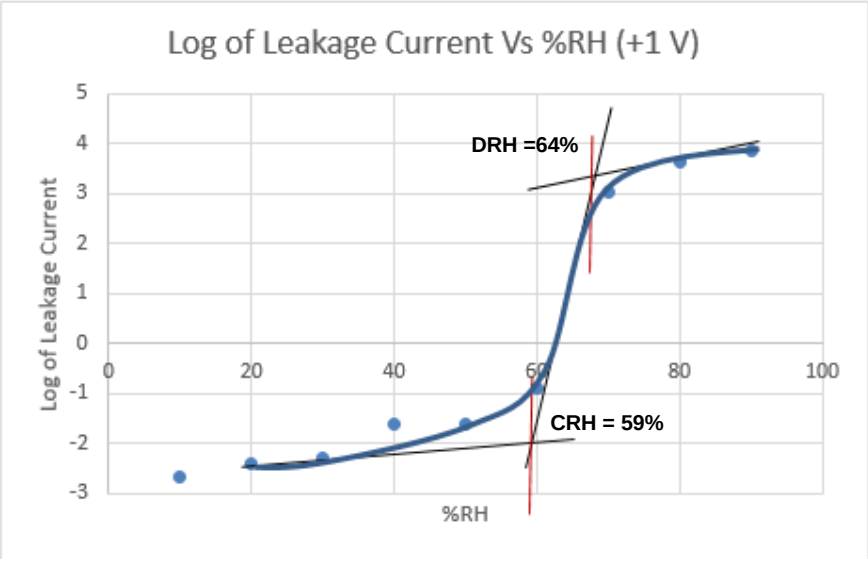

Figure 6-9 Logarithmic plot of Leakage Current versus %RH for NH_4NO_3 (+1 Volt)

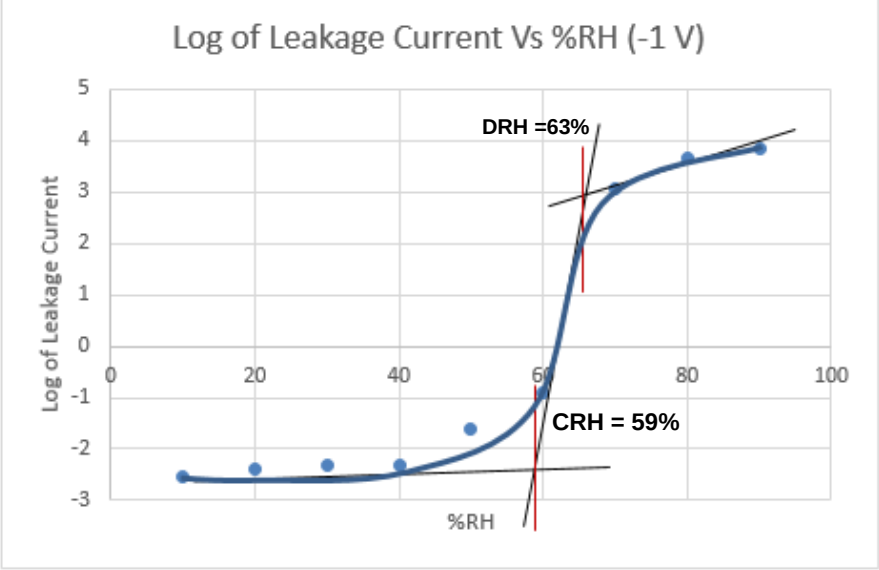

Figure 6-10 Logarithmic plot of Leakage Current versus %RH for NH_4NO_3 (-1 Volt)

The before and after pictures of the comb coupon dispensed with NH_4NO_3 solution is as seen in Figure 6-11 and Figure 6-12 depicts the effect of relative humidity in the presence of particulate contamination. The corrosion effects are also very evident.

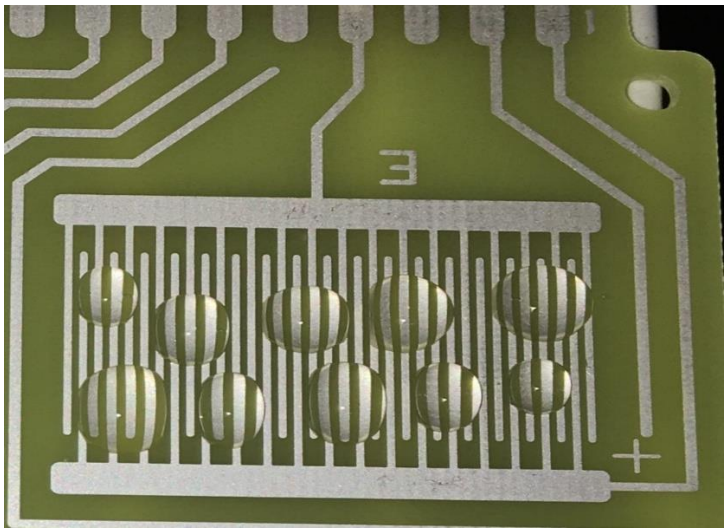

Figure 6-11 Drops of NH_4NO_3 dispensed on the comb coupon.

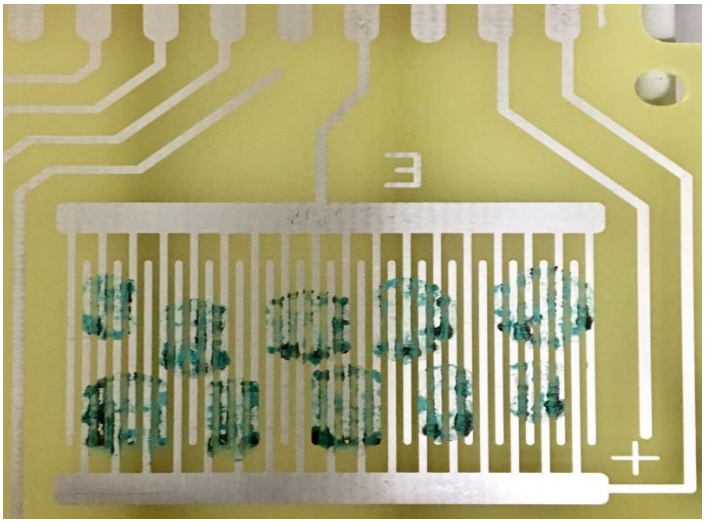

Figure 6-12 Corrosion due to the conducting nature of the NH_4NO_3 salt solution at a relative humidity higher than the DRH.

6.1.3 To estimate the DRH of Magnesium Chloride ($MgCl_2$)

Table 6-3 displays the values of leakage current obtained at various values of %RH on the application on +1V and -1V respectively to the magnesium chloride sample. The log of leakage current is also calculated and tabulated.

Table 6-3 Leakage current at varying values of %RH on the application of +1V and -1V ($MgCl_2$ Sample)

+ Volt			-1 Volt		
%RH	I (mA)	Log I	%RH	I (mA)	Log I
10	0.1	-2.30259	10	0.1	-2.30259
20	1.3	0.262364	20	1.2	0.182322
30	5.3	1.667707	30	4.6	1.526056
40	12.8	2.549445	40	12.8	2.549445
50	18.8	2.933857	50	20.2	3.005683
60	24.7	3.206803	60	25.8	3.250374
70	33.7	3.517498	70	34.8	3.549617
80	38.8	3.65842	80	40	3.688879
90	41.3	3.720862	90	42.4	3.747148

Figure 6-13 and 6-14 displays the linear plots of leakage current versus %RH for the magnesium chloride sample when +1V and -1V have been applied respectively.

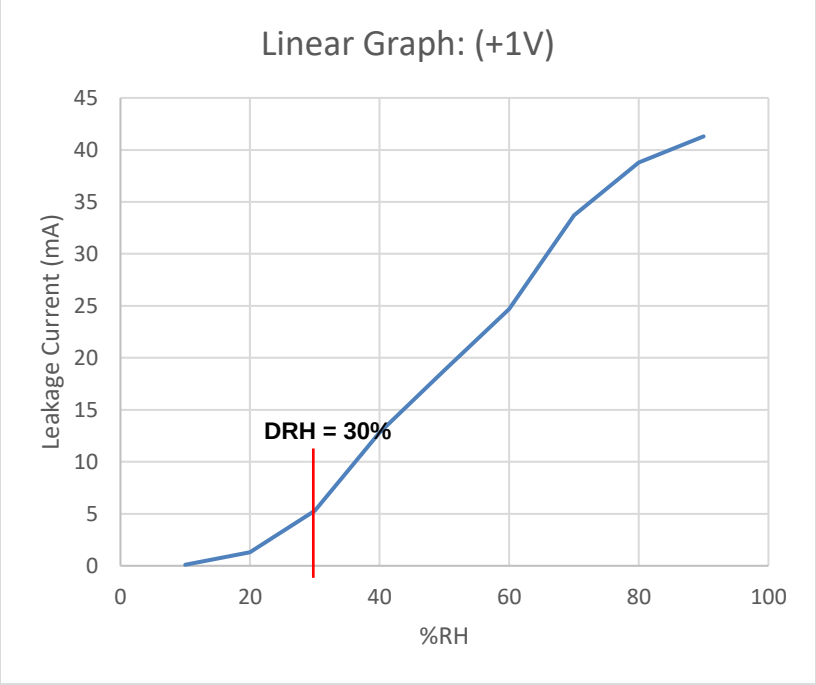

Figure 6-13 Linear plot of Leakage Current versus %RH for $MgCl_2$ (+1 Volt)

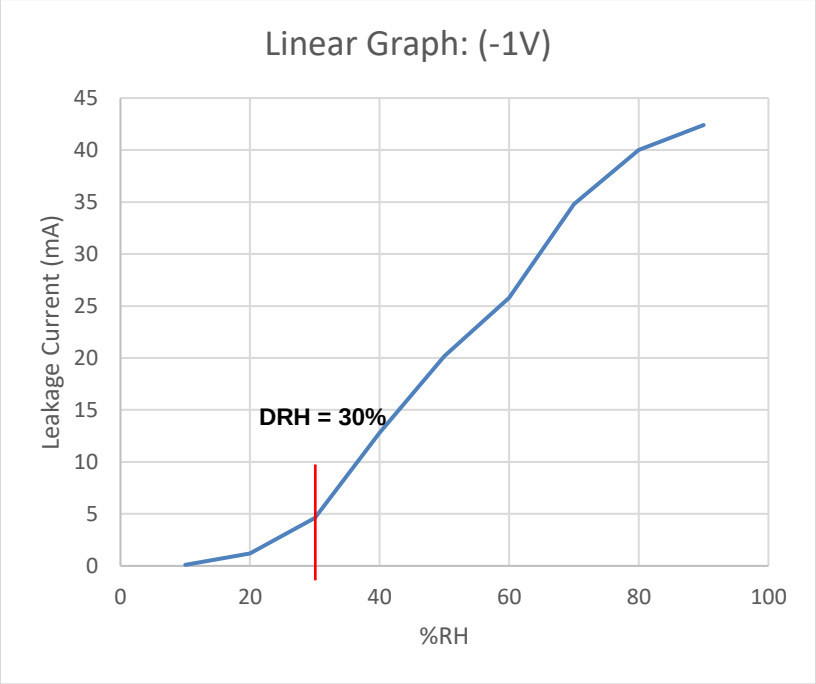

Figure 6-14 Linear plot of Leakage Current versus %RH for $MgCl_2$ (-1 Volt)

Figure 6-15 and 6-16 displays the logarithmic plots of leakage current versus %RH when +1V and -1V have been applied respectively.

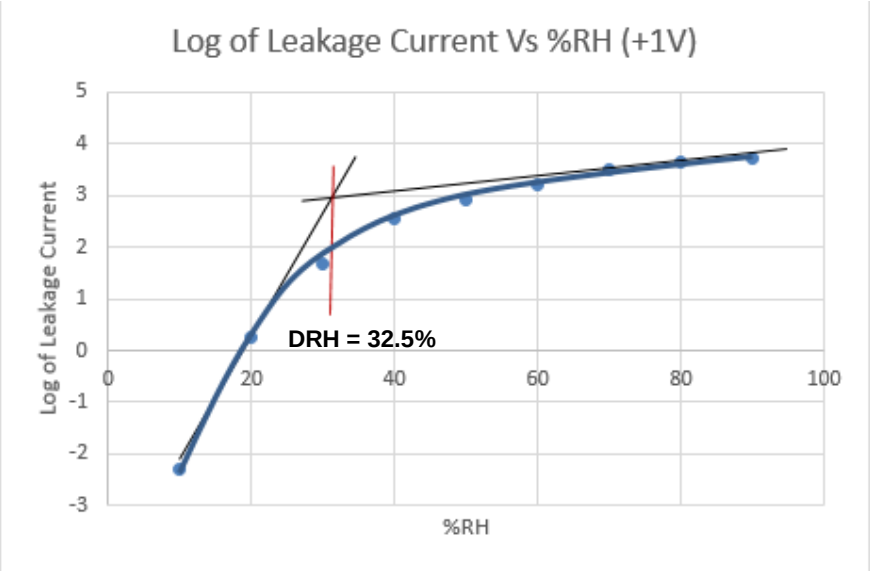

Figure 6-15 Logarithmic plot of Leakage Current versus %RH for $MgCl_2$ (-1 Volt)

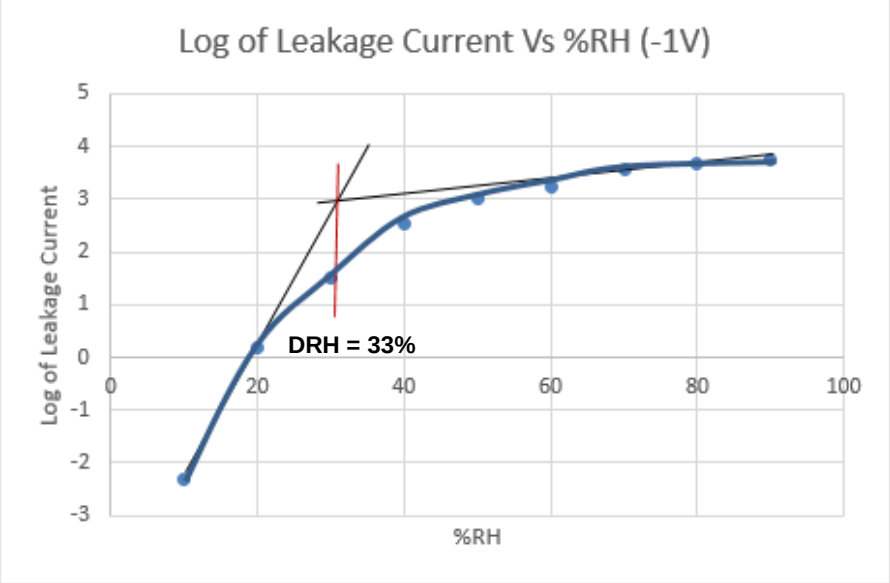

Figure 6-16 Logarithmic plot of Leakage Current versus %RH for $MgCl_2$ (-1 Volt)

The before and after pictures of the comb coupon dispensed with $MgCl_2$ solution is as seen in Figure 6-17 and Figure 6-18 depicts the effect of relative humidity in the presence of particulate contamination. The corrosion effects are also very evident.

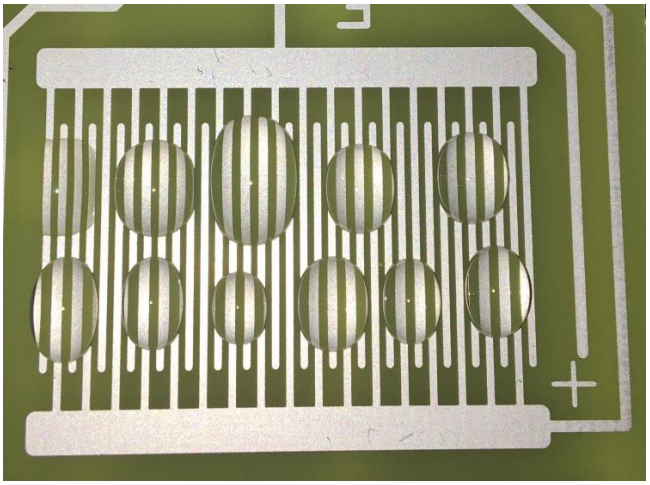

Figure 6-17 Drops of $MgCl_2$ dispensed on the comb coupon.

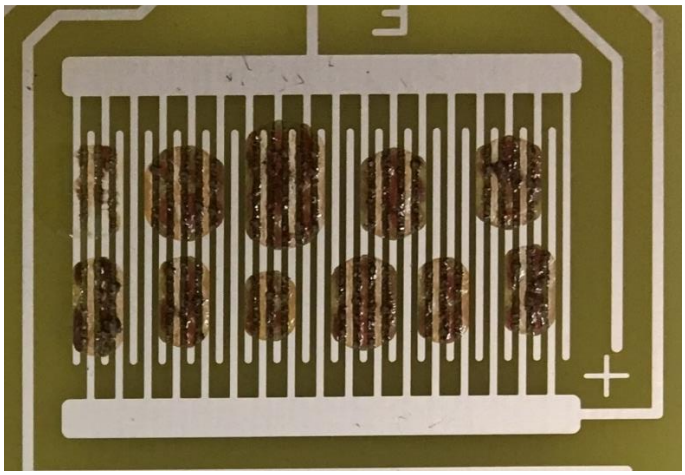

Figure 6-18 Corrosion due to the conducting nature of the $MgCl_2$ salt solution at a relative humidity higher than the DRH.

6.2 Discussions

From observing the linear plots for all the three salt samples Figures 6-1, 6-2, 6-7, 6-8, 6-13 and 6-14, it is rather tempting to interpret these linear plots in terms that the sudden increase in electrical conductivity (or leakage current) or the intercepts of the lower and higher humidity asymptotes being the deliquescence relative humidity of the salts. However, the main problem faced here is the obtained DRH values which are 70% for NaCl, 60% for NH_4NO_3 and 30% for $MgCl_2$ do not coincide with their published values as seen in Table 6-4. Also, they depend on the magnitude of the vertical scale.

Table 6-4 Comparison of experimental results with the published results by analyzing the linear plots of leakage current versus %RH

Salt	Published Values at 25^oC	Experimental Values (Linear Plots)
Sodium Chloride	DRH: 75.8%	DRH: 70%
Ammonium Nitrate	DRH:64%	DRH: 60%
Magnesium Chloride	DRH: 32.78%	DRH: 30%

In order to overcome this drawback and to obtain the deliquescence relative humidity with published values, another efficient method of plotting the values of leakage current are to be discovered.

The logarithm of leakage current is plotted against %RH as seen in Figures 6-3, 6-4, 6-9, 6-10, 6-15 and 6-16. The curves which are S-shaped can then be made piecewise linear by drawing straight lines the cover the inversion region, the lower relative humidity asymptote and higher relative humidity asymptote. The intersection of the lower relative humidity asymptote and the inversion line corresponds to the critical relative humidity (CRH) of the salt. It is at this value that the leakage current begins to rise sharply with the

increase in %RH. The intersection of the inversion line with the higher relative humidity asymptote corresponds to the deliquescence relative humidity (DRH) of the salt. At lower humidity ranges, the salt is generally in equilibrium with the humidity. Thus, a small increase in the relative humidity does not considerable change the electrical conductivity of the salt as the salt stays relatively dry. There is a rapid rise in the conductivity as the salt absorbs enough moisture to start approaching the deliquescence state. This can be noticed by the high slope of the inversion region. When the relative humidity continues to rise above the DRH of the salt, the salt is completely dissolved and any further rise in the relative humidity has very little influence on the electrical conductivity of the salt solution being tested. It is logical to consider the intercept of the inversion line and higher relative humidity asymptote to be the DRH of the salt because it refers to the value of relative humidity where the salt has absorbed just the right amount of moisture to become wet and that any further absorption of water will not cause an appreciable increase in its conductivity. Table 6-5 shows a comparison of the DRH of salts obtained performing the experiment, using logarithmic plots, with their published values. It is seen the experimentally obtained results perfectly match the published results thereby validating this experimental approach.

At higher relative humidity ranges, the SIR between the features on the coupon drastically decrease. The salt begins to conduct electricity and the images obtained after the experiment clearly displays the corrosion that takes place. Therefore, it would be efficient and judicious to maintain the relative humidity in a data center below the CRH of accumulated particulate matter to ensure the reliable operation of IT equipment and prevent its deterioration by electrical current leakages between the closely spaced features.

Table 6-5 Comparison of Experimental Values with Published Values

Salt	Published Values at 25°C	Experimental Values (Logarithmic Plots)
Sodium Chloride	CRH: 61% DRH: 75.8%	CRH: 61% DRH: 75.5%
Ammonium Nitrate	CRH: 59% DRH: 63%-64%	CRH: 59% DRH: 63%
Magnesium Chloride	DRH: 32.78%	DRH: 32.5%

Accumulated particulate matter with low deliquescence relative humidity is of major concern. It could either be generated in the data center space or outdoor air. In certain areas with poor air quality, most of the particulate matter obtain entry into the data center by the ventilation air that is driven through the HVAC (Heating, Ventilation and air-conditioning) systems.

Coarse and fine particulate matter in semi-urban and urban areas come from the exhaust of motor vehicles. The most polluting ones being those that are generated in diesel fueled vehicles. Diesel particulate matter, also known as DPM, is a particulate component of the diesel exhaust that released into the atmosphere, it can take the form of singular or individual particles. They are known as ultrafine particles because most of them are in the invisible submicron range of 0.1µm and are not visible to the naked eye. DPM includes diesel soot, aerosols such as ash particulates, sulphates, silicates and metallic abrasion particles.

ASHRAE Standard 52.2-2012 defines MERV as minimum efficiency reporting value [37]. MERV 8 and MERV 13 air filters are used to remove coarse and fine dust particles respectively from the outside air that is entering the data center. The control of DPM require MERV 16 or higher [37]. Data center that utilize CRAC units, the minimum filter that is required is MERV 8.

Fine and ultrafine particles that are present in the outdoor air or ambient have very high ionic content. The ionic content is in the form of ammonium salts, nitrate and sulphate [38-41]. Concerns with respect to fine dust with low deliquescence relative humidity on PCBs is well documented but cases of IT equipment failure due to fine dust have not been published yet.

Chapter 7

Conclusion

- To reduce power consumption and due to rapid expansion of the IT equipment business, data center operators should allow data centers to run using ASEs and also allow data centers to operate in the ASHRAE A1 allowable environment.
- The use of ASEs risks the entry of particle contaminants, both natural and anthropogenic, and should be controlled.
- Salts or dust has the tendency to absorb moisture, become wet and start conducting if the relative humidity in the data center rises above its DRH.
- In this study, an effective method to determine the DRH of dust is brought to light. The experiment is validated by determining the CRH and DRH of pure salts i.e NaCl, NH_4NO_3 and $MgCl_2$ and then comparing it with their published values.
- This method also proves to be an effective method in determining the CRH and DRH of salts and overcomes the limitations of the other measuring techniques.
- The current sensor can accurately measure upto 0.01mA making this a high precision technique.
- The entire setup is cost effective, very reliable and easy to handle.
- The process is also time efficient and one can obtain the DRH value of salts or dust quickly.
- This methodology can therefore be implemented to help lay a modus operandi of establishing the limiting value or an effective relative humidity envelope to be maintained at a real-world data center facility for its continuous and reliable operation at its respective location.

Chapter 8

Future Work

- To collect dust samples from various cabinet locations within a data center and employ this experimental technique to determine the DRH of dust or a mixture of salts.
- To study and understand the change in the trend of the graphs obtained for dust samples and pure salts.
- To determine an operating relative humidity envelope for the efficient, reliable and continuous operation of a data center specific to its location.
- CFD and Simulation tools can be employed by designing data centers with airside economizers having differ power densities and determining the path flow of airborne contaminants [42].
- Identifying the most susceptible regions of particulate deposition and developing effective mitigation strategies to eliminate particulate matter, thus preventing corrosion related failure. An initial study has been done [42,43].

References

[1] Shah JM, Awe O, Gebrehiwot B, et al. Qualitative Study of Cumulative Corrosion Damage of Information Technology Equipment in a Data Center Utilizing Air-Side Economizer Operating in Recommended and Expanded ASHRAE Envelope. ASME. J. Electron. Packag. 2017;139(2):020903-020903-11. doi:10.1115/1.4036363.

[2] ASHRAE Technical Committee 9.9, 2010, “ASHRAE DOE Course: Save Energy Now Presentation Series,” American Society of Heating, Refrigerating, and Air-Conditioning Engineers, Dallas, TX.

[3] Jimil M. Shah, "Reliability challenges in airside economization and oil immersion cooling", *The University of Texas at Arlington*, May 2016

[4] Thermal Guidelines for Data Processing Environments, ASHEAE Datacom Series, 3rd Edition, 2012, ASHRAE, Atlanta, GA, USA.

[5] J. Dai, D. Das, and M. Pecht, “Prognostics-Based Risk Mitigation for Telecom Equipment under Free Air Cooling Conditions”, Applied Energy, Volume 99, November 2012, pp 423–429.

[6] Intel Information Technology, “Reducing data center cost with an air economizer”, IT@Intel Brief; Computer Manufacturing; Energy Efficiency; Dec, 2008.

[7] R. P. Frankenthal, D. J. Siconolfi and J. D. Sinclair, “Accelerated Life Testing of Electronic Devices by Atmospheric Particles: Why and How”, J. Electrochemical Soc., Vol. 140, pp. 3129-3134, 1993

[8] ASHRAE, “2015 Supplement Energy Standard for Buildings Except Low-Rise Residential Buildings,” vol. 8400, 2015.

[9] "Air-Side Economizer," Energy Star, [Online]. Available: www.energystar.gov/index.cfm?c=power_mgt.datacenter_efficiency_economizer_airside.

[10] Cole, M., L. Hedlund. T; Kiraly, S. Nickel, P. Singh and T. Tofil, Harsh Environmental Impact on Resistor Reliability, SMTA Int'l Conf, Proc., 24 Oct 2010.

[11] Directive 2002/95/EC of the European Parliament and of the Council of 27 January 2003 on the Restriction of the use of Certain Hazardous Substances on Electrical and Electronic Equipment Official Journal L 037, February 13, 2003, 19-23.

[12] 6. Fu, H., C. Chen, P. Singh, J. Zhang. A. Kurella, X. Chen, X. Jiang, J. Burlingame and S. Lee, Investigation of Factors that Influence Creep Corrosion on Printed Circuit Boards," SMTA Pan Pacific Microelectronics Symposium, Kauai, 14-16 Feb 2012.

[13] Fu, H., C. Chen, P. Singh, J. Zhang. A. Kurella, X. Chen, X. Jiang, J. Burlingame and S. Lee, Investigation of Factors that Influence Creep Corrosion on Printed Circuit Boards, Part 2, SMTAI 2012.

[14] Jud Ready W.,1 L. J. Turbini, R. Nickel and J. Fischer, A Novel Test Circuit for Automatically Detecting Electrochemical Migration and Conductive, Journal of ELECTRONIC MATERIALS, Vol. 28, No. 11, 1999 Anodic Filament Formation

[15] Song B., M. H. Azarisn and M. G. Pecht, "Effect of temperature and relative humidity on the impedance degradation of dust-contaminated electronics," Journal of The Electrochemical Society, 160 (3), 2013, C97-C105.

[16] Seinfeld J. H. and S. N. Pandis, "Atmospheric Chemistry and Physics," John Wiley & Sons, Inc, New York, NY.

[17] Zhao P. et al. "Characteristics of concentrations and chemical compositions for PM2.5 in the region of Beijing, Tianjin and Hebei, China," Atmos. Chem. Phys. Discuss., Vol. 2013, 863-901.

[18] U. S. Environmental Protection Agency. *AIRTrends 1995 Summary – Nitrogen Dioxide (NO2).* ONLINE. 2014. Available: http://www.epa.gov/airtrends/aqtrnd95/no2.html [07 Oct. 2014].

[19] Comizzoli R. B.et al. “Corrosion of electronic materials and devices by submicron atmospheric particles,” The Electrochemical Society Interface, Fall 1993, 27-33.

[20] Y.N.Liang, J.G.Zhang and J.J.Liu, “Identification of inorganic compounds in dust collected in Beijing and their effects on electric contacts”, 43rd IEEE Holm Conference on Electric Contacts, Philadelfia, PA. USA. Oct.20-22,1997, 315-327

[21] Christofer Leygraf, Thomas E. Graedel, “Atmospheric corrosion”, John Wiley & Sons, Inc., ISBN 0-471-37219-6, 2000

[22] J.W. Wan, J.C. Gao, X.Y. Lin and J.G. Zhang, “Water-Soluble Salts in Dust and Their Effects on Electric Contact Surfaces”, Proceedings of the International Conference on Electrical Contacts, Electromechanical Components and Their Applications, Jun., 1999, 37-42

[23] P-E Tegehall, “Impact of Humidity and Contamination on Surface Insulation Resistance and Electrochemical Migration”, IVF Industrial Research and Development Corporation, http://www.europeanleadfree.net/

[24] ISA, 2013, “Environmental Conditions for Process Measurement and Control Systems: Airborne Contaminants,” ISA-The Instrumentation Systems, and Automation Society, Research Triangle Park, NC, Standard No. ISA-71.04- 2013.

[25] A DerMarderosian, "The electrochemical migration of metals," Proc. Int. Society of Hybrid Microelectronics, p.134, 1978.

[26] G. T. Kohman, H. W. Hermance, and G. H. Domes "Silver migration in electricalinsulation," Bell System Technical Journal vol. 34, pp. 11-15, 1955.

[27] G. Ripka and G. Harshyi, "Electrochemical migration in thick-film ICs," Electrocomp. Sci. Technol., vol. 11, p. 281, 1985.

[28] M. V. Coleman and A E. Winster, "Silver migration in thick-film conductors and chip attachment resins," Microelectronics Journal, No. 4, p. 23, 1981

[29] Singh P, Klein L, Agonafer D, Shah JM, Pujara KD. Effect of Relative Humidity, Temperature and Gaseous and Particulate Contaminations on Information Technology Equipment Reliability. ASME. International Electronic Packaging Technical Conference and Exhibition, *Volume 1: Thermal Management* (): V001T09A015. doi:10.1115/IPACK2015-48176

[30] Singh, P. P. Ruch, S. Saliba and C. Muller, Characterization, Prevention and Removal of Particulate Matter on Printed Circuit Boards, IPC APEX, San Diego, Feb 2015.

[31] Yang L., R. T. Pabalan and M. R. Juckett, “Deliquescence relative humidity measurements using an electrical conductivity method,” Journal of Solution Chemistry, Vol. 35. No. 4, April 2006, 583-604

[32] L. Yang, R. T. Pabalan, and L. Browning, Experimental Determination of the Deliquescence Relative Humidity and Conductivity of Multicomponent Salt Mixtures, in *Scientific Basis for Nuclear Waste Management XXV*, P. McGrail and G. A. Cragnolino, Eds. *Mater. Res. Soc. Symp. Proc.* 713, 135–142 (2002).

[33] Wexler A. and S. Hasegawa, Relative humidity-temperature relationships of some saturated salt solutions in the temperature range.

[34] M. Weekes, “PWB Contamination & Reliability DOE”, Proceedings of SMTA International Conference, Chicago, IL, September 2001.

[35] C. H. Hamann, A. Hamnett, and W. Vielstich, *Electrochemistry*, New York: Wiley-VCH, 1998.

[36] Adafruit INA219 Current Sensor Breakout [PDF File].

[37] ASHRAE Standard 52.2-2012, Method of testing general ventilation air-cleaning devices for removal efficiency by particle size, Atlanta, GA, USA.

[38] Harrison R.M., et al. “Airborne Particulate Matter in the United Kingdom.” Third Report of the Quality of Urban Air Review Group, May, 1996.

[39] Husar R., “Properties of Particulate Matter,” Washington University, St. Louis, 1999.

[40] Harrison R. and J. Yin, “Characterisation of Particulate Matter in the United Kingdom,” Report produced for Defra, the National Assembly for Wales, the Department of the Environment in Northern Ireland and the Scottish Executive, The University of Birmingham, March 2004.

[41] Čupr P., Z. Flegrová, J. Franců, L. Landlová, and J. Klánová, “Mineralogical, chemical and toxicological characterization of urban air particles,” Environment International 54 (2013), 26–34.

[42] Thirunavakkarasu. G, Saini. S, Shah J.M., Agonafer. D, "Air Flow Pattern and Path Flow Simulation of Airborne Particulate Contaminants in a High-Density Data Center Utilizing Airside Economization" ASME, INTERPACK 2018, San Francisco, California.

[43] Gautham Thirunavakkarasu, "Air Flow Pattern and Path Flow Simulation of Airborne Particulate Contaminants in a Cold-Aisle Containment High-Density Data Center Utilizing Airside Economization", *The University of Texas at Arlington,* May 2018.

Biographical Information

Roshan Anand received his Bachelor of Engineering degree in Mechanical Engineering from Reva Institute of Technology and Management, Bangalore, Karnataka, India, in 2015. Given his passion and innovative spirit, he decided to pursue his Master of Science in Mechanical Engineering at the University of Texas at Arlington in August 2016, believing that he had much to both offer and gain from the graduate program making his attendance there a good mutual fit. He has been a part of the Electronics MEMS and Nano electronics System Packing Center since October 2016. He was working on NSF I/UCRC projects for 'Energy Efficient Data Centers' and also studying the 'Effect of Particulate Contamination in Data Centers' over the course of his graduate study. His passion and research interests have always been in the fields of Machine Design and Simulation, Composite Structures, Solid and Structural Mechanics and Electronic Packaging.